



The University of Akron
College of Engineering

Senior Design Project

Spring 2019

Final Report

Zips Formula Electric Race Car

Cooling System

Project Advisor

Dr. Daniel Deckler

Project Members

Marcus Caddiell

Nick Crane

Rania Hemaia

Viktor Lozitsky

Abstract

The Zips Electric team was able to design a car for the 2019 year from the ground up. One of the sub-systems for the car included the cooling system. The task for this senior design project was to improve on the previous cooling design attempt. We set out to reduce the number of radiators from two to one while retaining the effectiveness of the system. This report details the calculations necessary in order to choose the proper components for the system. Also, design choices were made using many engineering methods that we learned in our Concepts of Design course, such as weighted decision matrices and structure diagrams. An exhaust venting system was also designed to ensure proper airflow through the radiator. The components associated with the system ducting were 3D printed and had to be designed accordingly.

Acknowledgment

As a group, we wanted to give special acknowledgments to those who made this project possible. The University of Akron's college of Engineering was instrumental in making this whole car coming together. Dr. Deckler also provided an irreplaceable guiding hand in this project as our project advisor. We also have Dr. Gross, a former professor at the University of Akron, to thank for literature on the design of a cooling system. Finally, we would like to extend our gratitude to the entire team that worked diligently together to complete this first car on time.

Table of Contents

Abstract	1
Acknowledgment	2
Table of Contents	3
Introduction	3
Technical Analysis	4
Chapter 1: Design Brief	4
Chapter 2: Conceptual Design	6
Chapter 3: Embodiment Design	9
Chapter 4: Detailed design	Error! Bookmark not defined.
Chapter 5: Discussion	41
Chapter 6: Conclusion	Error! Bookmark not defined.
References	43
Appendices	44

Introduction

The Zips Formula Electric race car is an opportunity for students to use in-class knowledge on a project. This car has many subsystems, all of which are necessary for the car to make it competition and race. These subsystems include, but are not limited to: structural frame, composites, suspension, steering, accumulator, brakes, and our cooling system. The subsystem that our group was tasked with working on was the cooling system for the car.

The purpose of the cooling system is to cool several components of the electric car. These components include the battery inverter and the motor driving the car. As in any system, there are inefficiencies from the power inversion and use of this power in the motor. These inefficiencies present themselves as heat losses. The main purpose of the cooling system was designed to keep these different components at proper operating temperatures.

A cooling system consists of a radiator with high-temperature hosing connecting to the inverter and motor. To complete the hose path was a pump with proper flow rate and ability to overcome pressure loss. Added to this, a fan was connected to the back of the radiator. This insures air flow at low speed application. The final part of the design was the venting system. This ensures proper flow of air. It was important to design this vent system in the allotted space.

The cooling system for the previous year's car did not have much though behind it. There were two radiators and our project started with reducing that number to only one radiator. To aid in designing the system, engineering techniques such as weighted decision matrices, structure diagrams and Failure Mode and Effects Analysis charts were used. This ensured choosing the correct components and designs for our applications along with a system that was safety minded.

Chapter 1: Design Brief

There were many design aspects to consider when designing a cooling system for an electric car. One of the important design improvements we wanted to do was reduce the number of radiators. This required calculation of the cooling load the radiator would experience with only one radiator.

To aid with design of this system, we used different methods learned in Concepts of Design class. These included function diagrams, morphological charts and FMEA (failure mode and effects analysis).

Team standards were followed for choosing components. Here, one of the important aspects is to have all of the low voltage systems on the same 12V system. This caused some early-on design changes to the pump and fan.

Pump and Fan Selection

These calculation included looking into the flowrate of water and air. Good water flow rate was necessary when selecting a pump. Another design aspect that went into choosing the pump was pressure drop across the cooling system. Different components cause a drop in pressure. If this drop in pressure is not overcome, the system is not able to pump through the system. For low speeds, the flow rate of air was found from the fan specifications. These flow rates were factored into heat transfer equation of the radiator.

Radiator Selection

All calculation were done using a radiator previously used in last year's electric car. Important dimensions were found and used from this radiator included length and width. Also, the number of fins and fin diameters were found from this radiator. The radiator was found to be sufficient for cooling the car for the Formula Electric team. The previous system did not look into this aspect and used at "overkill" system with two radiators. Using the calculation as justifying, we were able to remove one of the radiators.

Guidelines had to be followed for any car competing at a Formula Electric event. This included the cooling liquid that can be used, which was water. Next, the electric and cooling systems had to be separated from the driver by a firewall. Finally, a catch can had to be integrated into the design. This can had to be capable to hold at least 10% of the total fluid used in the system. The cooling liquid may not leak any liquids when tilted at a 45 degree angle. This includes the water from our system.

Chapter 2: Conceptual Design

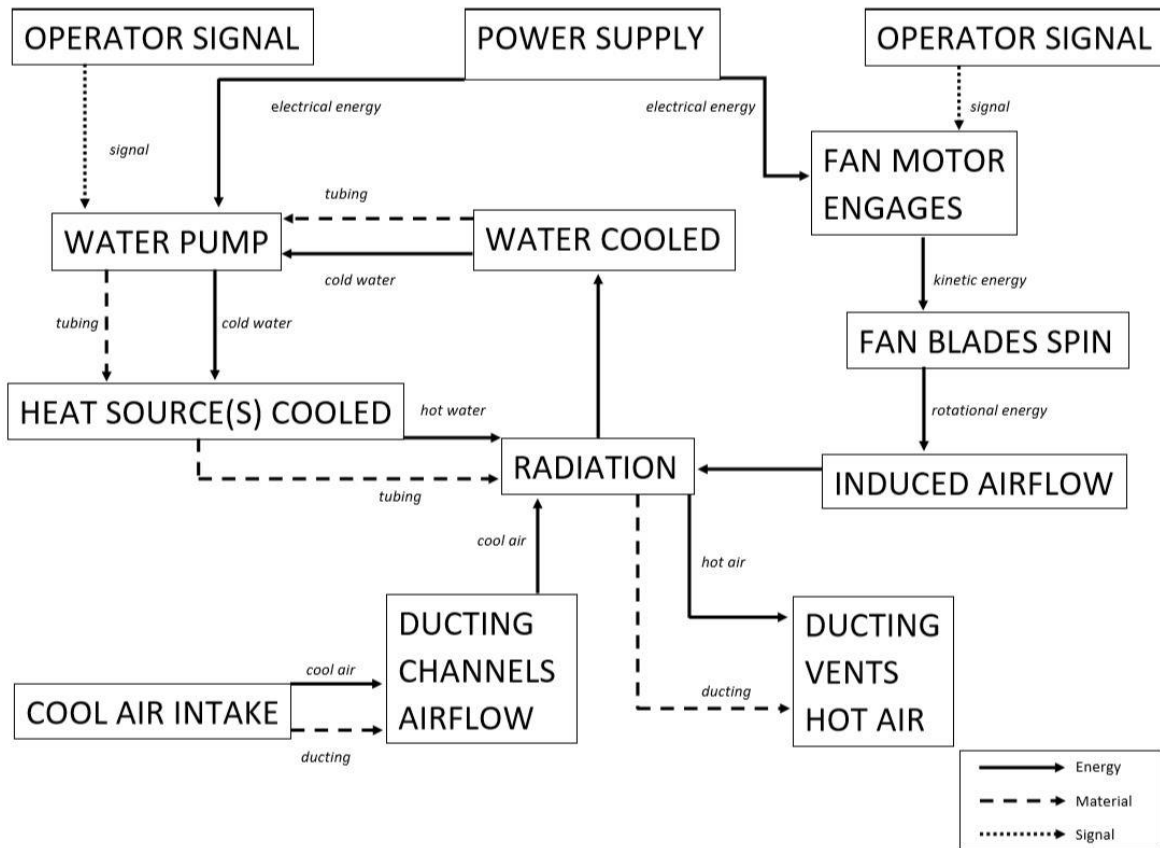


Figure 1: Cooling System Structure Diagram

The purpose of the structure diagram is so that we are able to see the big picture when it comes to the cooling system. This system is actually a sub-system in a very complicated car. Also, we rely on many other teams for things such as where the system fits in the frame as well as how the pump and fan will be powered. The structure diagram helps visualize how the numerous other systems fit together, possible interference and improvements that can be done.

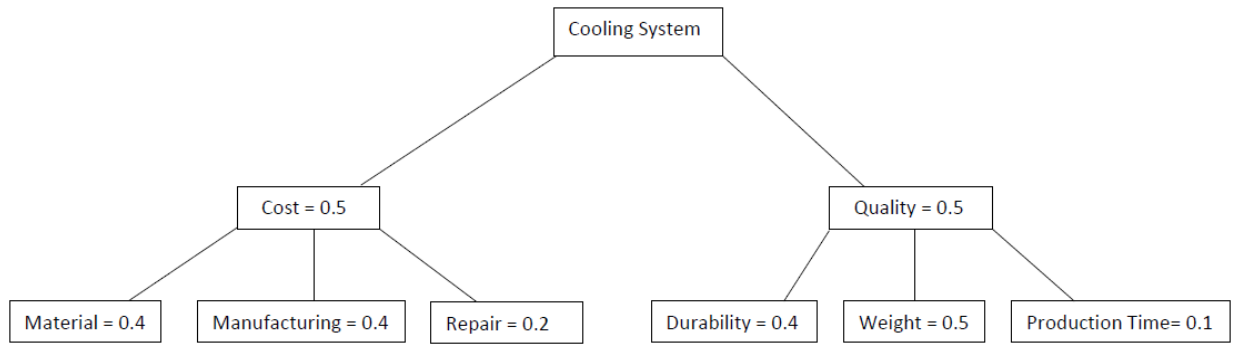


Figure 2. *Cooling System Objective Tree*

A weighted decision matrix is a very helpful tool when choosing between different designs or components. This is done by first creating an objective tree which breaks down the criteria regarding how each decision was made. These will be split up by weight. Adding all the weights will equal one. This allows a designer to have more weight on more important aspects. Next, a rating between 1 and 10 is assigned to each component. Multiplying the rating and weight will give each design a score. Added the scores compares overall design of each. Using the weighting factor and rating correcting will help choose which design is best. All 6 weighted decision matrices that we utilized to choose between different options are listed in Appendix G.

One way these are useful is when choosing between different designs. A decision matrix was done for the venting design. When looking at all the different designs, each had different positives and negatives. Things we compared included design, safety, air flow/restriction, installation and the amount of 3D printing needed. Design was important since every aspect of the car receives points for design at competition. Safety had to deal with where the hot exhaust air exited in relation to the driver. Air flow took the shape of the vent and how air could navigate through. Installation took into account whether modification had to be done to the body paneling. Finally, it was taken into consideration how hard the part would be to 3D print and ultimately how much it would cost.

Table 1: Weighted decision matrix for ductwork

Vent Weighted Decision Martix								
Evaluation Criteria		Weighting Factor W(i)	Concept 1		Concept 2		Concept 3	
			V(i) (Rating)	V(i)*W(i)	V(i) (Rating)	V(i)*W(i)	V(i) (Rating)	V(i)*W(i)
1	Design	0.25	9	2.25	9	2.25	8	2
2	Safety	0.25	7	1.75	5	1.25	7	1.75
3	Air Flow	0.2	6	1.2	9	1.8	3	0.6
4	Installation	0.15	3	0.45	10	1.5	3	0.45
5	Printing Amount	0.15	7	1.05	3	0.45	9	1.35
		$\Sigma W(i)=1$	$\Sigma W(i)*V(i)=$	6.7	$\Sigma W(i)*V(i)=$	7.25	$\Sigma W(i)*V(i)=$	6.15

Table 2: Criteria for the ductwork

Criteria	Significance
Design	Design is judged at competition and is important to
Safety	The safety was judge on where hot exhaust gases left in relation to the driver
Air Flow	The over design evaluated whether air had choke points or elbows
Installation	Whether or not body panel would have to be modified to install
Printing Amount	Printing amount directly ties with how much it would cost and how feasible it would be to print

For the pump, we had two comparable pumps. The main difference here was the pricing between them. In the end, we made the decision to buy the more expensive and more efficient pump. We felt as though the increased system efficiency outweighed the extra cost.

Table 3: Weighted decision for water pump selection

Pump Weighted Decision Martix						
Evaluation Criteria		Weighting Factor W(i)	EBP40 Electric Booster Pump		EPB23 Electric Booster Pump	
			V(i) (Rating)	V(i)*W(i)	V(i) (Rating)	V(i)*W(i)
1	Flow Rate	0.3	8	2.4	6	1.8
2	Pressure Loss	0.3	8	2.4	3	0.9
3	Price	0.25	5	1.25	7	1.75
4	Size	0.15	5	0.75	7	1.05
		$\Sigma W(i)=1$	$\Sigma W(i)*V(i)=$	6.8	$\Sigma W(i)*V(i)=$	5.5

Table 4: Criteria for water pump selection

Criteria	Significance
Flow Rate	Flow volume was judged in comparison to the system needs
Pressure Loss	Water pressure was judged in comparison to the system needs
Price	How expensive the pump was in relation to how much we expected
Size	How the pump fits in the designated space the cooling system had

The choice for the tubing had many different factors. Some of the factors included were whether they were specialized to what we were doing with the cooling system. For example, some tubing had poor pressure and temperature ratings. Another factor was the ease of use. The system needs to be flexible. This will help in the future with installation and removal at competition.

Table 5: Weighted decision matrix for the tube selection

Tubing Weighted Decision Martix								
Evaluation Criteria		Weighting Factor W(i)	High Temp Scillicon Rubber		CPVC		Aluminum Piping	
			V(i) (Rating)	V(i)*W(i)	V(i) (Rating)	V(i)*W(i)	V(i) (Rating)	V(i)*W(i)
1	Coolant Flow	0.25	5	1.25	5	1.25	7	1.75
2	Temp Capability	0.25	10	2.5	6	1.5	8	2
3	Price	0.15	8	1.2	10	1.5	3	0.45
4	Ease of Use	0.15	10	1.5	10	1.5	1	0.15
		$\Sigma W(i)=1$	$\Sigma W(i)*V(i)=$	6.45	$\Sigma W(i)*V(i)=$	5.75	$\Sigma W(i)*V(i)=$	4.35

Table 6: Criteria for the tube selection

Criteria	Significance
Coolant Flow	Chance to kink and how fittings was assessed
Temp Capability	How the tubing fits the specific needs of a cooling system
Price	How the tubing fits the specific needs of a cooling system
Ease of Use	Ease of instillation and ease to improve system if needed

Chapter 3: Embodiment Design

Many aspects of embodiment design were used in implementing this cooling system. It was important to understand the frame layout and to know how much room we had for the cooling system. After completing the system, a function structure diagram and failure mode and effects (FMEA) chart were used to assess the cooling system for possible ways in which it might fail.

Each one had an important role in decisions that we made, ensuring proper design and preventing possible causes of failure in our system.

Frame Layout

The radiator cannot be located on the outside of the cabin of the vehicle, such as in the combustion vehicle. This is because the accumulator causes the mid-section of the frame to be built wider, and any extra width would negatively impact the aerodynamics of the car. Thus, we are left with the only option of placing the radiator within the frame.

Last year the car attempted to implement two radiators within the cooling system, located on both sides of the frame. With the decision to reduce the number of radiators to one, we were left with the decision to place the radiator on either the left or right side of the frame. We decided to place the radiator on the left side of the frame based on the fact that only one radiator side has a cap. This decision substantially reduced the total length of tubing needed, which in turn reduced the amount of water needed, the weight, and the cost of the system. **Figure 3**, below, depicts the available space within the frame in which the cooling system can be placed.

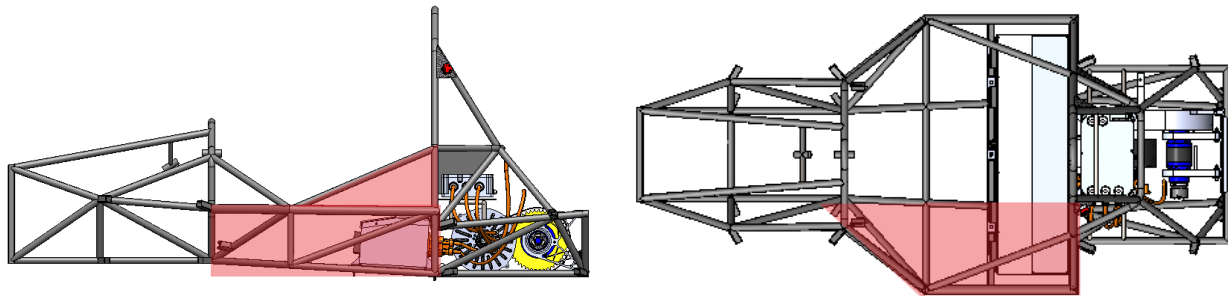


Figure 3: *Layout of available space within the cars frame*

We were given roughly 1.014 ft³ of frame space to design a functional cooling system. Since the radiator is located within the frame, next to the driver, FSAE has many rules in place to protect the driver in case of an accident. Per FSAE rules the cooling system must be fully enclosed by a firewall which isolates the system from the cabin of the car. The car seat, which is in the center of the frame and firewall, extends diagonally from the edge of the seat. This reduces the amount of space available to fit the cooling system in.

Along with the size constraints, the cooling system also must adhere to multiple specifications. The required specifications are as follows:

Motor Specifications

- Cooling Medium: 8 LPM at 50°C
- Pressure Drop: 0.9 Bar
- Max inlet Pressure: less than or equal to 2 Bar

Inverter Specifications

- Coolant Flow Rate: 8-12 LPM
- Pressure Drop: 0.3 Bar at 8 LPM

FSAE Specifications

- Electric motors and HV electronics must use plain water with no additives or oil as the coolant
- Catch can must have a minimum volume of 10% of the fluid being contained
- Catch can must be vented

FMEA

A Failure Mode and Effects chart, or FMEA, helps list all parts of the cooling system and the possible causes of failure. The severity of failure and possibility (occurrence) of failure are assessed on a 1 to 10 scale. Detection of is also scored this scale. This number reflect how easy detection is for each mode of failure. The Risk Proximity Number (RPN) is assessed by multiply the severity, occurrence and detection. The RPN reflects how important each possible mode of failure is. Depending on the RPN, further action many need to be done to insure safe use. **Figure 4** below elaborates such ranking.

Item	Function	Potential Mode Failure	Potential Effects of Failure	Severity	Potential Causes of failure	Occurrence	Current Design Control (Prevention)	Current Design Control (Detection)	Detection	RPN	Recommended Action
Radiator	Cooling the inverter and motors of electrical vehicle	Inadequate cooling	Car overheating	7	Puncture from outside object	2	Screening in front of radiator	Screening must be checked	1	14	No action needed
Fan	Helps air move through radiator and venting especially at low speeds	Fan turns off because of loss of power or failure	Car overheating at low speeds	3	Loss of power or defective fan	1	Wires have been checked and secured	Audible sound of fan needs to be heard	4	12	Low risk is associated with the fan but checks need to be done
Venting	Give a path for air to move to the radiator and out the rear of the car	Not air-tight	Not efficient cooling	1	Not properly sealed	3	Sealer was applied	Check sealer	3	9	No action needed
Hose	High temperature hosing delivered the water to be cooled from the inverter, to the motor, to the radiator	Leaking or disconnection of the hose	Un-Efficient cooling	5	Slowly losing coolant or coolant spraying out	1	High-Temperature hosing was used	Visual Checks of Cooling System before and after driving	3	15	Checks need to be done
Connections	Connections link the radiator, inverter and motors. This insures a closed system	Leaking or disconnection of the hose	Not efficient cooling	5	Slowly losing coolant or coolant spraying out	1	All connections were checked. Hosing is zip-tied to secure location	Visual Checks of Cooling System before and after driving	3	15	Checks need to be done

Figure 4: Failure mode and evaluation analysis chart

Chapter 4: Detailed design

Due to limited space within the frame, the Mishimoto Radiator was a good fit for the space available. This was the same radiator used in the previous car's cooling system. The main improvement we wanted to accomplish was reducing the number of radiators from two to one. Many calculations had to be done to insure that this design change could be made. Not only did this center around the radiator, but it was also important that the pump, fan and vent system were properly designed for our application in the electric car. The calculations started with the cooling load experienced from heat given off of the motor and inverters. The radiator had to ensure that the motor and inverter temperature stayed within the range for optimum performance. Since the endurance race at competition is the physically demanding and generates the most amount of heat at a given time, it is used as a basis to determine the cooling load. From the resulting cooling load we then found the heat transfer rate, the efficiency, and heat capacity ratio of the radiator. Only after these calculation, we were able to determine if the radiator was sufficient or not.

Cooling Load Calculations

To determine the cooling load needed, we start by finding the energy and the time to complete the constant velocity cornering, also the acceleration, deceleration and max velocity portions of the straight sections in one lap of the endurance course. Since our team will be competing in the Nebraska competition this year, the endurance course from 2012 was selected to do these calculations. **Figure 5** below show such track.

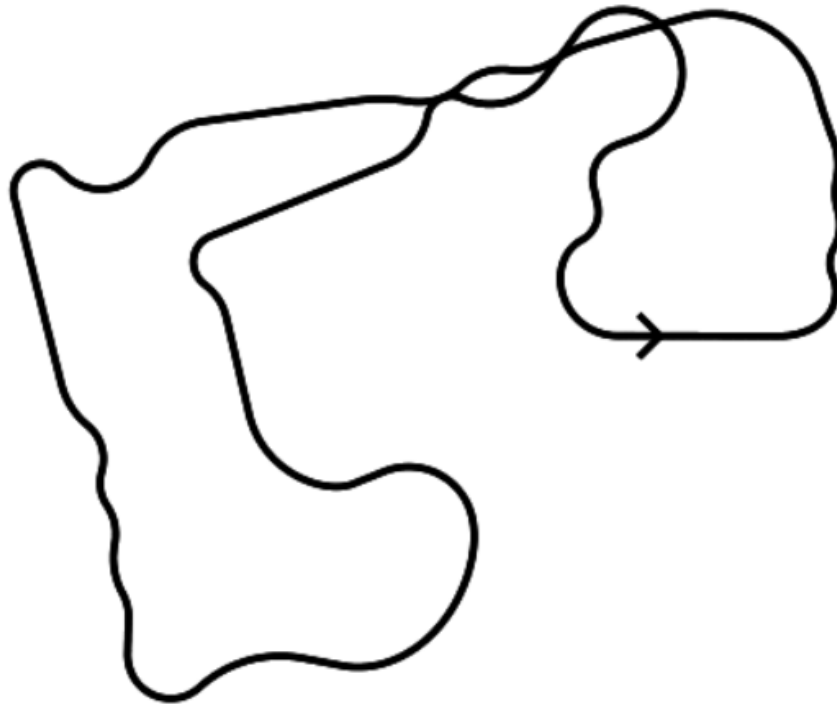


Figure 5: *FSAE Endurance Course, Nebraska 2012*

The total length of this track is roughly 1.2 km (0.7 mi) and consists of 40 turns and/or slaloms with 13 straight sections. Following the same methodology as the book we will assume all acceleration and braking occur in straight sections of the track and all corners are pure cornering with no acceleration and/or braking. The Formula SAE vehicle has a mass of $m = 510 \text{ lbm}$ and $m = 655 \text{ lbm}$ (297 kg), with a 145 lb driver (for calculations purposes). The tires can develop a maximum lateral force of $\sum F_{LAT} = 1113.5 \text{ lb}$ (5244N) for pure cornering. The vehicle has a frontal area of $A_f = 1.045 \text{ m}^2$, a drag coefficient of $C_D = 0.75$, and the tires have a rolling resistance coefficient, $C_{RR} = 0.025$. The drivetrain efficiency, $\eta_{DT} = 0.91$. The air mass density is $\rho_A = 1.21 \frac{\text{kg}}{\text{m}^3}$. The maximum average coefficient of braking, $\mu_A = 1.8$ for all four

tires. The Gear Ratio, $GR = 3.51$, the tire radius, $R_T = 0.254m$ the Slip Ratio, $SR = 0.1$ the Braking Acceleration, $a_B = 17.658 \frac{m}{s^2}$. We assume the steering angles of the two front tires are equal and use a representative value of $\theta = 10^\circ$

The calculations are broken down into the different sections of the track. First, the energy required to navigate each turn and/or slalom is determined. This is done by first calculating the cornering velocity, V_i using the equation,

$$V_i = \sqrt{\frac{R \sum F_{LAT}}{m}}$$

Where R is the radius of the turn. Next, the time to navigate this corner is found from,

$$t_i = \frac{S_i}{V_i}$$

Where S_i is the length of the turn. Finally, the Energy required for constant velocity cornering can be found using the equation,

$$E_{Vi} = \left(\frac{1}{2} \rho_{AIR} A_F C_D V_i^2 + C_{RR} W V_i + (F_{LLF} + F_{LRF}) \sin \theta V_i \right) \frac{t_{Vi}}{\eta_{DT}}$$

Where F_{LLF} is the lateral force on the left front tire, F_{LRF} is the lateral force on the right front tire and since these values were specifically given we estimate $(F_{LLF} + F_{LRF})$ term in the above equation as equal to $\frac{\sum F_{LAT}}{2}$ The results from these calculations are summarized in Appendix F,

Table App.F.1.

In order to analyze the acceleration phases, we will need the engine torque as a function of the engine speed, the drive train gear ratios, the drive tire radius, and an estimate of the tire slip ratio for acceleration. **Figure 6** below is the extrapolated results of the engine torque as a function of engine speed, obtained from the manufacturer's graph, in located Appendix C, **Figure App.C.3.**

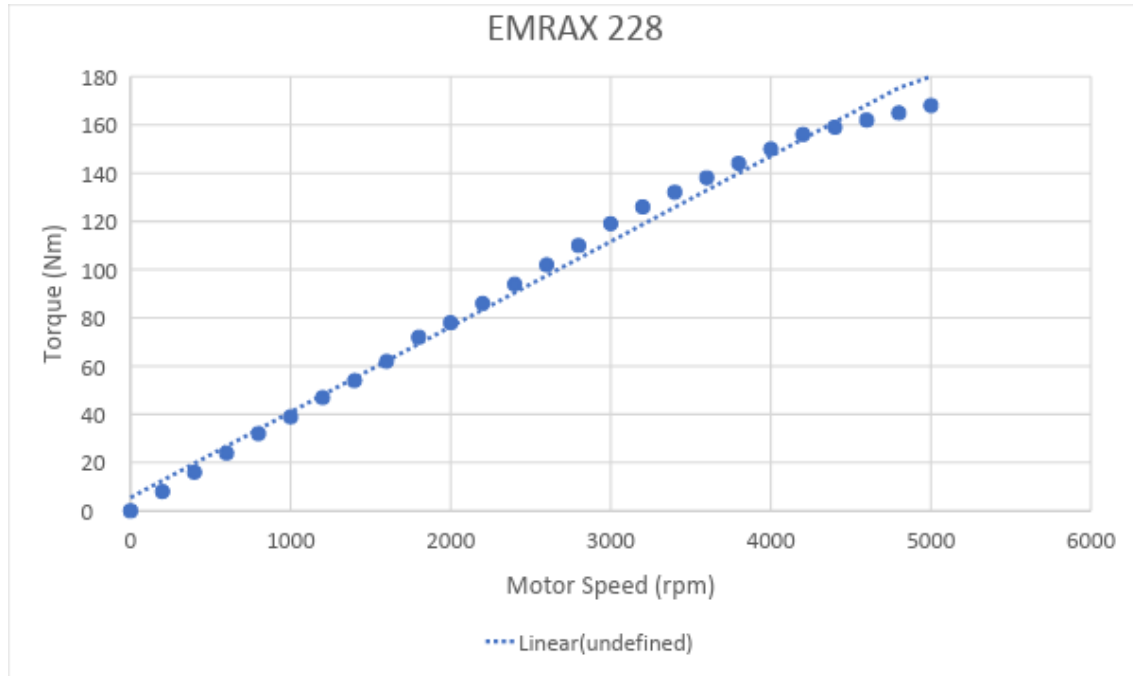


Figure 6: *Torque and Horsepower Curve for EMRAX 228*

The curve above was poly fitted to obtain an equation that can be used to determine the average rear axle torque at any given engine speed. The equation obtain is as follows,

$$T_{RA} = (-2 \times 10^{-6} N^2 + 0.0468N - 3.6001)GR\eta_{DT}$$

The vehicle average acceleration for the average rear axle torque

$$a_A = \frac{T_{RA}}{R_T m}$$

Next, the time and energy required in the straight line sections of the endurance course. The constant cornering velocity of the prior corner is the initial velocity while the final velocity depends on the length of the straight section. The Emrax 228 is a sequential motor, which means it has no gears. Therefore, the maximum attainable velocity obtained in each straight section depends on the driver's skill level and ability to enter these sections with highest velocity possible. Acceleration time need in each section is found from,

$$t_{iA} = \frac{(V_{iMAX} - V_i)}{a_A}$$

The acceleration distance is

$$S_{iA} = V_i t_{iA} + \frac{1}{2} a_A t_{iA}^2$$

The engine energy required to accelerate the vehicle from velocity V_a to velocity V_b

$$E_{iA} = \frac{1}{2\eta_{DT}} \left(m + \frac{C_{RR}W}{a_A} \right) (V_b^2 - V_a^2) + \frac{\rho_{AIR} A_F C_D}{8\eta_{DT} a_A} (V_b^4 - V_a^4)$$

The braking time is found from

$$t_{iB} = \frac{(V_{iMAX} - V_i)}{a_B}$$

The braking distance is

$$S_{iB} = V_{iMAX} t_{iB} - \frac{1}{2} a_B t_{iB}^2$$

The maximum velocity distance in a section is given by the equation

$$S_{iViMAX} = (S_i - S_{iA} - S_{iB})$$

The maximum velocity time in a section is

$$t_{iViMAX} = \frac{S_{iViMAX}}{V_{iMAX}}$$

The maximum velocity engine output energy

$$E_{iViMAX} = \left(\frac{1}{2} \rho_{AIR} A_F C_D V_{iMAX}^3 + C_{RR} W V_{iMAX} \right) \frac{t_{iViMAX}}{\eta_{DT}}$$

To obtain an achievable maximum velocity in each straight section, this value was determined by manipulating the value until the maximum velocity distance was the lowest possible number. The results of these calculations are in Appendix F, **Table 2a and 2b**. Once the output engine power was found, the motor efficiency, η , equation can be manipulated to find the electrical input power,

$$P_{in} = \frac{P_{out}}{\eta_{DT}}$$

The power loss of the engine is essential turned into heat and can be considered the required cooling load of the system. This cooling load can be found using the equation,

$$CL = P_{IN} - P_{OUT}$$

Table 1 below, is the tabulated results of the total energy expended, average engine power developed, and average torque and engine speeds while navigating the corners and straights of the endurance track. The efficiency of the motor during this time was determined using the motor efficiency map in Appendix C, **Figure App.C.3**, with the average values of torque and engine speed. The overall efficiency of 87.36% was determined by multiplying the drivetrain efficiency by the motor efficiency. Using the above equations for the input power with this efficiency the required radiator cooling load for one lap of the endurance track was determined.

Table 7: Overall results of one complete lap of the endurance course.

Total Time	60.406 s
Total Energy Expended	1014253.114 Nm
Average Engine Power	16.7905 kW
Average Torque	105.991 Nm
Average Engine Speed	2725.2905 rpm
Motor Efficiency	96%
Overall Efficiency	87.36%
Input Power	19.2199 kW
Cooling Load	2.4294 kW

When the car accelerates it generates the greatest amount of heat, so as a conservative estimate the power dissipated in the straight selection will be used. The results of these calculations are in the **Table 8** below.

Table 8: Results from the straight portions of the track

Straight Energy	527937.4675 Nm
Straight Time	15.5055 s
Average Energy	34.0484 kW
Average Torque	113.0377 Nm
Average engine speed	2909.6470 rpm
Motor Efficiency	96%
Overall Efficiency	87.36%
Input Power	38.9748 kW
Cooling Load	4.9264 kW

These cooling load calculations are track dependent and will increase or decrease depending on the length of the track, the number of turns and/ or slaloms, and number of straight sections featured in the track.

Heat Transfer Calculations

Heat transfer analysis is necessary to be able to evaluate the heat transfer throughout our system. It is necessary to know the rate of heat transfer and cooling load which the radiator provides. The heat transfer in our system takes place between a radiators with hot coolant coming into contact with cooler, outside air. Every radiator is unique in its ability to cool based on numerous factors. These not only include outside dimensions of a radiator but also how the fins of the radiator are laid out. The next section explains equations used in calculating the heat transfer through the radiator. Note that the radiator is analyzed as a heat exchanger device. The equations used here can be used to apply the cooling load associated with the electric can and the heat transfer resulting. Table 3 below shows basic dimensions of the radiator we analyzed.

Table 9: Measured dimensions of the radiator

Core Height	0.2403 m
Tube Width	0.0022 m
core width	0.1082 m
fin height	0.0079 m
length of tube	0.0201 m
tube width	0.0016 m
tube thickness	0.0003 m
inside length	0.0195 m
diameter	0.01702 m
# of tubes	20

Heat Transfer Rate, \dot{Q} :

$$\dot{Q} = U_o A_o F LMTD$$

Where:

$$U_o = \text{Overall Heat Transfer Coefficient} = \frac{1}{R_o + R_{wall} + R_i}$$

$$A_o = \text{outside surface area of the water tube} = 1.1735 \text{ m}^2$$

$$F = \text{Correction Factor (assumed} = 1)$$

$$LMTD = \text{Log Mean Temperature Difference} = \frac{(T_{w \text{ In}} - T_{air \text{ Out}}) - (T_{w \text{ out}} - T_{air \text{ In}})}{LN \left(\frac{T_{w \text{ In}} - T_{air \text{ Out}}}{T_{w \text{ out}} - T_{air \text{ In}}} \right)}$$

Overall Heat Transfer Coefficient, U_o :

$$U_o = \frac{1}{R_o + R_{wall} + R_i}$$

In calculating the convective thermal resistance of the air flowing across the radiator, R_o , we first calculate average Nusselt number, Nu_{air2} , as follows:

$$Nu_{air2} = 1.86 \left[\frac{Re_{air2} Pr_{air2}}{\left(\frac{L_{air2}}{D_{hair2}}\right)} \right]^{1/3} = 1.86 \left[\frac{368.79 * 0.708}{\left(\frac{0.240 \text{ m}}{0.00164 \text{ m}}\right)} \right]^{1/3} = 2.4443$$

Outside (air) convective heat transfer coefficient, h_o :

$$h_o = \frac{k_{air2} Nu_{air2}}{D_{hair2}} = \frac{0.02753 \frac{W}{m \cdot ^\circ C} * 2.4443}{0.00164 \text{ m}} = 40.956 \frac{W}{m^2 \cdot ^\circ C}$$

Air thermal resistance, R_o , is:

$$R_o = \frac{1}{h_o} = \frac{1}{40.956 \frac{W}{m^2 \cdot ^\circ C}} = 0.024416 \frac{m^2 \cdot ^\circ C}{W}$$

Note: Air properties such as Prandtl number, Pr_{air2} , and thermal conductivity, k_{air2} , are obtained from **Figure App.B.3** in Appendix B of this report for air at 320 K.

Moving on to calculating the wall conductive thermal resistance, R_{wall} , we first collect the following data:

Inside surface area of water tube, $A_i = 0.18709 \text{ m}^2$

Outside surface area of water tube, $A_o = 1.1735 \text{ m}^2$

Thickness of fin, $t_{wall} = 0.0003 \text{ m}$

Thermal conductivity of Aluminum fin, $k_{wall} = 240 \frac{W}{m \cdot ^\circ C}$ (obtained from **Figure App.B.2** in Appendix B, at 100 °C)

Conductive thermal resistance of the radiator's walls, R_{wall} , is as follows:

$$R_{wall} = \frac{A_o t_{wall}}{A_i k_{wall}} = \frac{1.1735 \text{ m}^2 * 0.0003 \text{ m}}{0.1899 \text{ m}^2 * 240 \frac{W}{m \cdot ^\circ C}} = 7.84 \times 10^{-6} \frac{m^2 \cdot ^\circ C}{W}$$

In calculating the inside (water) thermal resistance, R_i , we first start by calculating the Nusselt number, Nu_{w2} :

$$Nu_{w2} = \frac{\left(\frac{f_{w2}}{8}\right) (Re_{w2} - 1000)(Pr_{w2})}{1 + 12.7 \left(\frac{f_{w2}}{8}\right)^{1/2} (Pr_{w2}^{2/3} - 1)} = \frac{\left(\frac{0.0442}{8}\right) (3170.8 - 1000)(1.75)}{1 + 12.7 \left(\frac{0.0442}{8}\right)^{1/2} (1.75^{2/3} - 1)} = 14.715$$

Inside (water) convective heat transfer coefficient, h_i :

$$h_i = \frac{k_{w2} Nu_{w2}}{D_{hw2}} = \frac{\left(0.6791 \frac{W}{m^{\circ}C}\right) (14.715)}{(0.002886 m)} = 3461.60 \frac{W}{m^2 \text{ } ^{\circ}C}$$

Note: Prandtl number, Pr_{w2} , and thermal conductivity, k_{w2} , of water are obtained for water at 100 °C from **Figure App.B.1** in Appendix B.

Now, the inside, water, thermal resistance is as follows:

$$R_i = \frac{A_o}{A_i h_i} = \frac{1.1735 m^2}{0.1899 m^2 * 3461.60 \frac{W}{m^2 \text{ } ^{\circ}C}} = 0.001812 \frac{m^2 \text{ } ^{\circ}C}{W}$$

Therefore, *Overall Heat Transfer Coefficient*, U_o , is as follows:

$$U_o = \frac{1}{R_o + R_{wall} + R_i} = \frac{1}{0.024416 \frac{m^2 \text{ } ^{\circ}C}{W} + 7.84 \times 10^{-6} \frac{m^2 \text{ } ^{\circ}C}{W} + 0.001812 \frac{m^2 \text{ } ^{\circ}C}{W}} \\ = 38.115 \frac{W}{m^2 \text{ } ^{\circ}C}$$

Notice that the air thermal resistance, R_o , is by far the greatest of other, water and wall thermal resistances.

Heat Transfer Rate Calculation

$$\dot{Q} = \dot{m}_w C_{p_w} (T_{w \text{ In}} - T_{w \text{ Out}})$$

$$\dot{Q} = \dot{m}_{air} C_{p_{air}} (T_{air \text{ out}} - T_{air \text{ in}})$$

Mass flow rate of water, \dot{m}_w , and air, \dot{m}_{air} , is:

$$\dot{m}_w = \left(\frac{12 L}{min}\right) \left(\frac{1 m^3}{1000 L}\right) \left(\frac{1 min}{60 sec}\right) \left(\frac{1000 kg}{1 m^3}\right) = 0.2 \frac{kg}{s}$$

$$\dot{m}_{air} = (0.2403 m)(0.1082 m) \left(3 \frac{m}{s}\right) \left(1.21 \frac{kg}{m^3}\right) = 0.09438 \frac{kg}{s}$$

Note that the mass flow rate of water and air are calculated for specific flow rate and velocity, respectively, however these values change when the care is in motion. **Figure 7**, and **Figure 8**, below show the water and air mass flow rates for various flow rates and velocities, respectively.

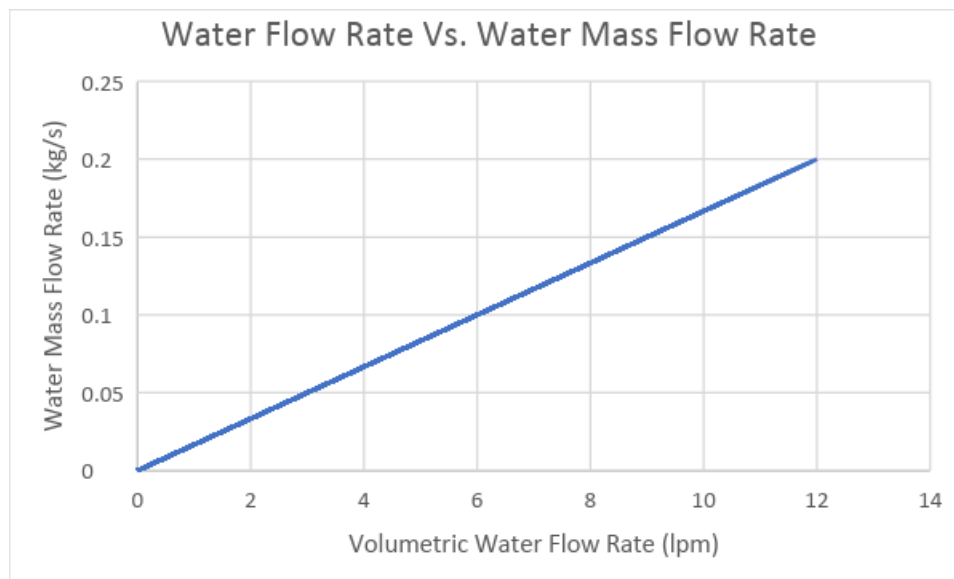


Figure 7: Water mass flow rate as a function of water volumetric flow rate

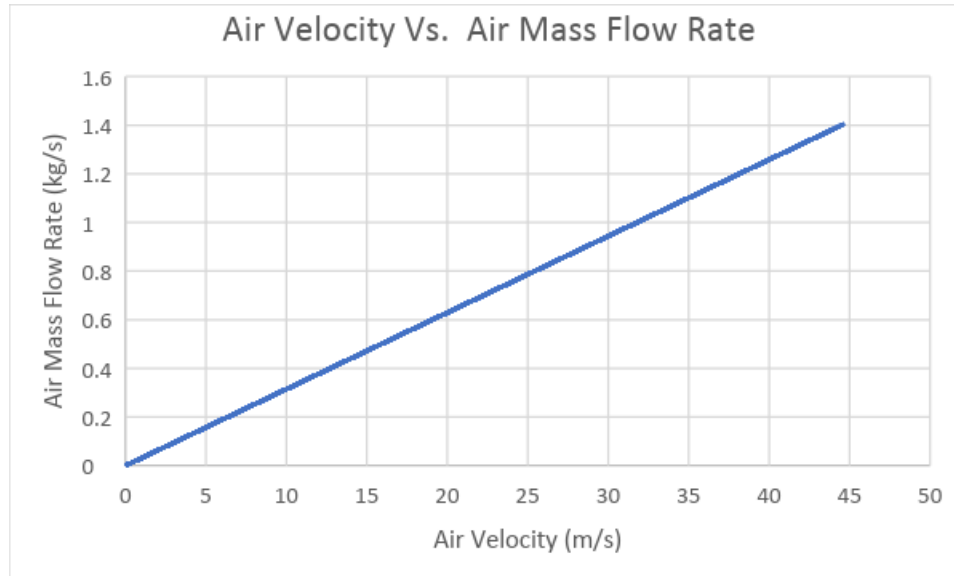


Figure 8: Air mass flow rate as a function of air velocity

Note: As velocity of air increases, mass flow rate of air increases as well, which leads to more air flow through radiator fins causing more heat loss and therefore better cooling.

Also, specific heat of water and air are obtained from **Figure App.B.1** and **Figure App.B.3**, respectively, where $C_{pw} = 4216 \frac{J}{kg \cdot ^\circ C}$ and $C_{p\text{air}} = 1008 \frac{J}{kg \cdot ^\circ C}$.

Assume

$$T_{w\text{ In}} = 100 \text{ }^\circ\text{C}$$

$$T_{\text{air In}} = 25 \text{ }^\circ\text{C}$$

cooling load was previously solved for in the section above as $\dot{Q} = 4926.4 \text{ W}$

Solving for by applying the mass conservation principle, we get

$$T_{w\text{ out}} = 50 \text{ }^\circ\text{C}$$

$$T_{\text{air Out}} = 76.78 \text{ }^\circ\text{C}$$

Note that temperature of exiting air is not constant, rather, it depends on the mass flow rate of air. **Figure 9** below expresses the temperature of exiting air as a function of the mass flow rate of air.

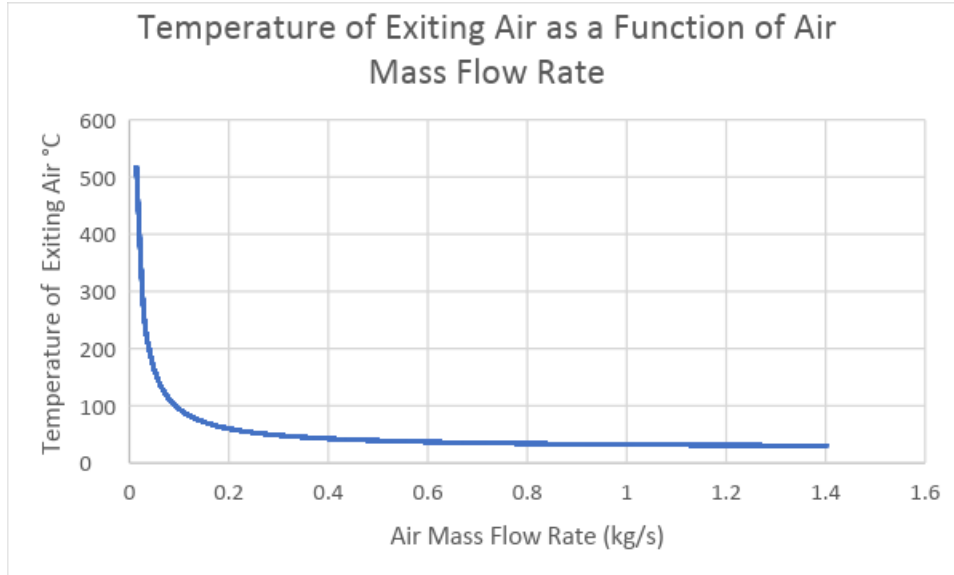


Figure 9: *Exiting air temperature as a function of air mass flow rate*

Note: as the mass flow rate of air increases due to increasing velocity, the temperature of air exiting the radiator decreases, which results in better cooling.

NOW: Heat Transfer Rate, \dot{Q} :

$$\dot{Q} = U_o A_o F LMTD$$

$$\dot{Q} = \left(32.979 \frac{W}{m^2 \cdot ^\circ C} \right) (1.1735 m^2) (1) \left(\frac{(100^\circ C - 76.78^\circ C) - (50^\circ C - 25^\circ C)}{LN \left[\frac{100^\circ C - 76.78^\circ C}{50^\circ C - 25^\circ C} \right]} \right) = 1077.82 W$$

$$= 1.077819 KW$$

Efficiency, P :

$$P = \frac{T_{air\ out} - T_{air\ in}}{T_{w\ in} - T_{air\ in}} = \frac{76.78^\circ C - 25^\circ C}{100^\circ C - 25^\circ C} * 100 = 69.05\%$$

Since temperature of exiting air is not constant, the efficiency and capacity ratio will vary. **Figure 10** and **Figure 11** show the efficiency and capacity ratio as functions of heat transfer rate respectively.

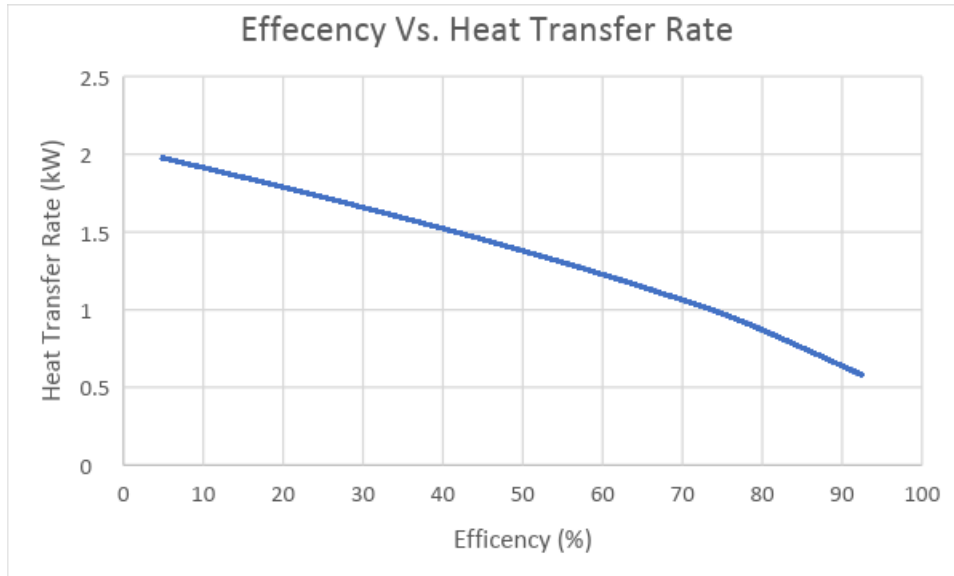


Figure 10: *Efficiency as a function of heat transfer rate*

Note: that the efficiency increases as the heat transfer rate decreases.

Capacity Ratio, R:

$$R = \frac{T_{w\ in} - T_{w\ out}}{T_{air\ out} - T_{air\ in}} * 100 = \frac{100\ ^\circ\text{C} - 50\ ^\circ\text{C}}{76.78\ ^\circ\text{C} - 25\ ^\circ\text{C}} * 100 = 96.56\ %$$

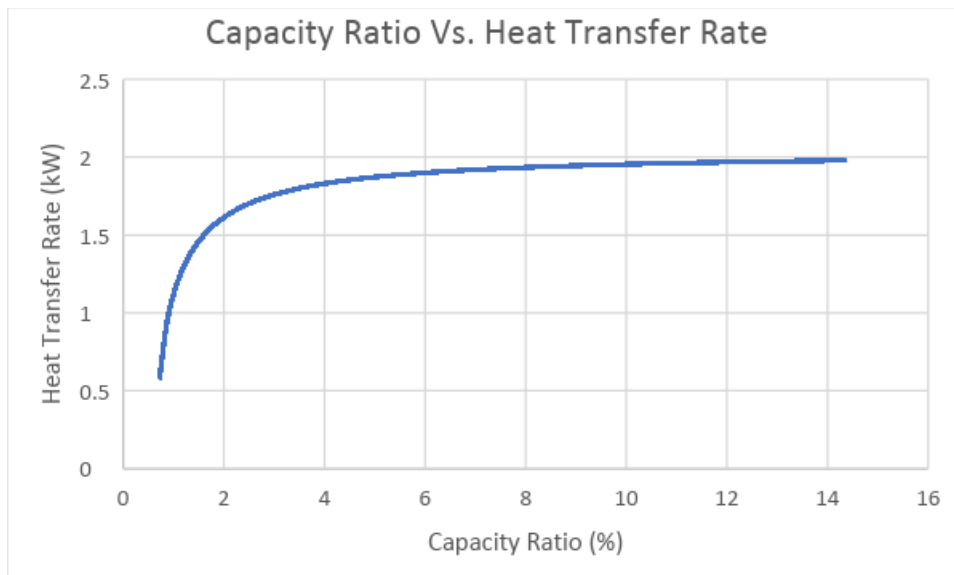


Figure 11: *Capacity ratio as a function of heat transfer rate*

Note: that the increasing heat transfer rate results in increasing capacity ratio.

Radiator Placement

The constraints for placement for the radiator was mainly centered around how it would best fit into the space allowed by the tube frame. Inside edge of the frame, the radiator sits at roughly at 60° . The idea would be a 90° but this was the closed we could achieve with the space allowed. Mounting tabs were manufactured and welded onto the frame to hold the radiator in this position (Drawings in Appendix E).

Due to space constraints and interference with the firewall, a 90° angle fitting had to be used on the inlet of the radiator and a 180° fitting on the outlet. These were put in place to avoid kinks from forming in the tubes and disrupting the flow. All types of fittings introduced into a system like this creates pressure and flow losses of some magnitude. The solution we came up with to minimize the total amount of losses was to move the inlet and outlet barbs on the radiator to its back face. **Figure 12** below depicts the change in location of these barbs. The new outlet of the radiator, located closer to the accumulator, still required a 45° angle fitting. This minimized the angle which the tube bends in from.

Fan Selection

We choose a 5.2" SPAL puller fan. The puller configuration of the fan was chosen since they are known to be better suited for application like a radiator. This type of fan is able to pull air through and from around the radiator. The venting system was design around the fan and radiator to minimize an air leaking.

Air Duct Design

With the location of the radiator decided now came the task to determine a proper way to duct the air through the radiator and out of the car. One feature that we wanted was for the fan to be housed within the ductwork. Again, due to space constraints the exhaust portion of the ductwork needed go above the accumulator. With the radiator sitting at a 60° angle we wanted to ensure that the inlet of the duct be tangent with the frame tubes to avoid interference with the body panels. To have the most amount of air flow through the radiator, the inlet needed to as wide as possible. **Figure 13** depicts the multiple design iterations of the ductwork. The inlet of each design remains the same and how the fan is housed remains the same. the exhaust portion of the duct changes with each iteration.



Figure 13: *Ductwork design one*

Figure 13 shows the first iteration of the duct design. The exhaust portion features an elbow that vents the hot air of the upper side of the car. The end is tangent with the frame tube and is cut to accommodate the radius in the body panel. This design requires a hole to be cut into the body panel.



Figure 14: *Ductwork design two*

Figure 14 shows the second iteration of the duct design. The exhaust portion features two pieces that vent the hot air out of the back of the car. The diameter of the duct slightly reduces before it deforms to fit into the triangle made by the frame tubes. This design does not require any hole to be cut into any of the body panels.



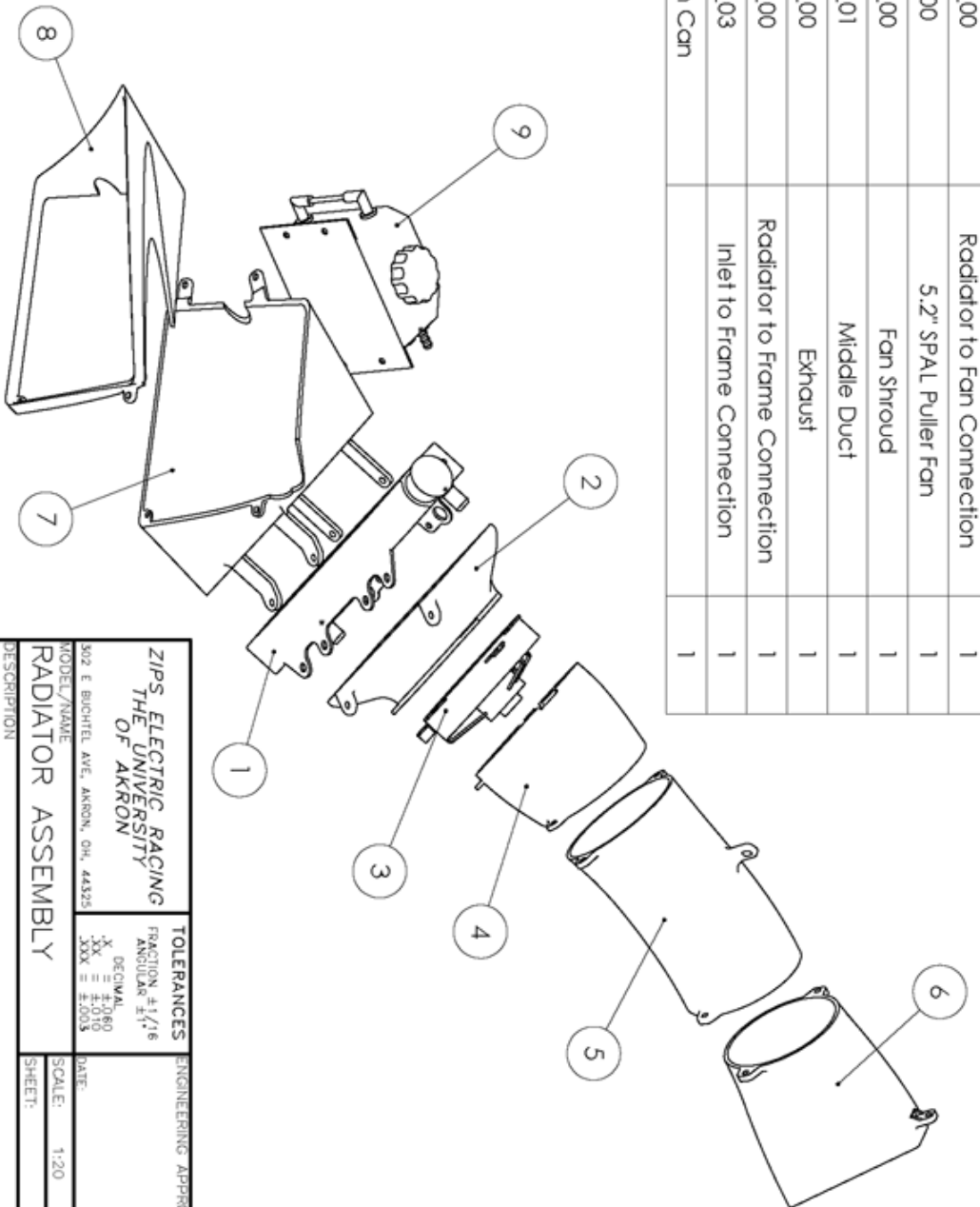
Figure 15: *Ductwork design three*

Figure 15 shows the third iteration of the duct design. The exhaust portion features an elbow that vents hot air out of the lower side of the frame. The elbow's diameter reduces significantly before it becomes tangent with the frame tube. This design requires a hole to be cut into the body panel.

Per FSAE, rule the accumulator must be taken out of the car to charge. Therefore, ductwork design two's exhaust portion will need to be taken in and out with the accumulator. Unlike design two, ductwork designs one and three were made to so that the exhaust portion did not have to be taken out along with the accumulator. However, the downside to these designs is that the elbow portion could potentially choke the flow.

In order to maintain the best airflow through radiator, i.e. maximize the air cooling potential, we choose to go with design two. Having to take the exhaust portions of the duct in and out with the accumulator was determined to be worth it. Since we have a design in mind, the next task is to choose what material and how we are going to make it. Multiple duct mounting tabs manufactured and welded onto the frame to hold these duct pieces in place (Drawing in Appendix E). **Figure 16** below is an exploded view of the radiator assembly that shows the connections between the duct pieces, radiator, and fan.

ITEM NO.	PART NUMBER	DESCRIPTION	Default/ QTY.
1	P801_01	Mishimoto Radiator	1
2	M802_00	Radiator to Fan Connection	1
3	P803_00	5.2" SPAL Puller Fan	1
4	M803_00	Fan Shroud	1
5	M805_01	Middle Duct	1
6	M806_00	Exhaust	1
7	M801_00	Radiator to Frame Connection	1
8	M804_03	Inlet to Frame Connection	1
9	Catch Can		1



ZIPS ELECTRIC RACING THE UNIVERSITY OF AKRON		TOLERANCES	
502 E BUCHTEL AVE, AKRON, OH, 44325 MODEL/NAME RADIATOR ASSEMBLY		FRACTION ±1/16 DECIMAL .XX ±.000 .XXX ±.003	ENGINEERING APPROVAL:
DESCRIPTION RADIATOR ASSEMBLY		SCALE: 1:20	DATE:
SHEET:		SHEET:	

Figure 16: Radiator Assembly

Air Pressure Drop across Radiator

After the duct dimensions have been finalized we were able to do calculations to determine the pressure drop across the radiator. Air pressure drop across the radiator depends mainly on the velocity which the car is moving. Other factors which affect air pressure drop are the loss coefficients at the inlet and exit of the duct. **Figure 17** below demonstrates the flow of air across the radiator fins. Section 1 shows the air entrance to the radiator fins. Section 2 is the actual radiator fins and section 3 is the area to which air exits.

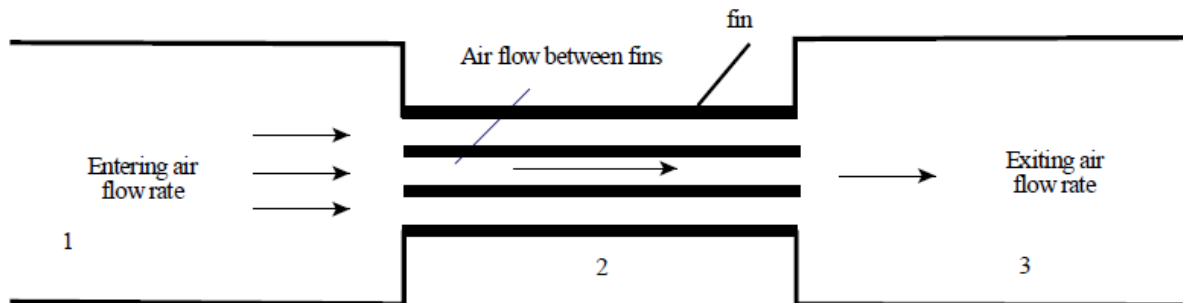


Figure 17: *Demonstrative model of air flow through the radiator fins*

Calculations of the find area of the radiator geometry must first be determined in order to proceed with the pressure drop calculations.

Upstream flow area of air channels, $Area_{air1}$:

$$Area_{air1} = Area_{air3} = 0.24028m * 0.10280m = 0.025999 m^2$$

Frontal area of tubes, $Area_{tubes\ frontal}$:

$$Area_{tubes\ frontal} = 0.24028m * 0.002159m * 20 = 0.010375 m^2$$

Frontal area of fins, $Area_{fins\ frontal}$:

$$Area_{fins\ frontal} = 0.007874m * 0.0001016m * 20 * 22 = 0.000351 m^2$$

Flow area of air channels, $Area_{air2}$:

$$Area_{air2} = 0.025999 m^2 - 0.010375 m^2 - 0.000351 m^2 = 0.01527 m^2$$

Air channel average velocity, V_{air2} :

$$V_{air2} = (V_{air1}) \left(\frac{Area_{air1}}{Area_{air2}} \right) = \left(3 \frac{m}{s} \right) \left(\frac{0.025999 m^2}{0.01527 m^2} \right) = 5.1072 \frac{m}{s}$$

Where V_{air1} is an assumed velocity of the approaching air.

$$\begin{aligned} fin \ slanted \ height &= \sqrt{(fin \ height)^2 \left(\frac{fin \ spacing}{2} \right)^2} = \sqrt{(0.00787 m)^2 \left(\frac{0.00184 m}{2} \right)^2} \\ &= 0.0079279 m \end{aligned}$$

Air channel hydraulic diameter,

$$D_{hair2} = \frac{4 Area_{air2}}{P_{air2}} = \frac{4 \left[\frac{1}{2} (0.00787 * 0.00184) \right]}{0.00184 + 2(0.0079279)} = 0.001643 m$$

The Reynolds number for the air flow, Re_{air2} :

$$Re_{air2} = \frac{V_{air2} D_{hair2}}{\nu_{air2}} = \frac{5.1072 \frac{m}{s} * 0.001643 m}{1.79 \times 10^{-5} \frac{m^2}{s}} = 468.79$$

Note that the flow is laminar; however, it will change as the velocity of air entering the radiator does.

The ratio of relative roughness of aluminum to the air channel hydraulic diameter:

$$\frac{\varepsilon}{D_{hw2}} = \frac{0.0000015 m}{0.001643 m} = 0.00091295$$

The air friction factor over the air channels, f_{w2} :

$$f_{air2} = \frac{64}{Re_{air2}} = \frac{64}{468.79} = 0.13652$$

The entrance and exit loss coefficients for the air channel, $k_{entrance}$ and k_{exit} , are respectively determined as follows:

$$k_{entrance} = 0.80$$

Note: The value of the entrance loss coefficient is obtained from **Figure App.A.3** in Appendix A for a reentrant entrance condition.

The momentum correction factor at point 2, β_2 , and the kinetic energy correction factor at point 2, α_2 , are respectively calculated as follows and used in calculating the exit loss coefficient, k_{exit} .

$$\beta_2 = \frac{2}{w V^2} \int_0^{\frac{w}{2}} (6V)^2 \left[\frac{1}{4} - \frac{y^2}{w^2} \right]^2 dy = \left(\frac{72}{w} \right) \left(\frac{w}{60} \right) = \left(\frac{72}{0.2286} \right) \left(\frac{0.2286}{60} \right) = 1.20$$

And

$$\alpha_2 = \frac{2}{w V^3} \int_0^{\frac{w}{2}} (6V)^3 \left[\frac{1}{4} - \frac{y^2}{w^2} \right]^3 dy = \left(\frac{432}{w} \right) \left(\frac{w}{280} \right) = \left(\frac{432}{0.2286} \right) \left(\frac{0.2286}{280} \right) = 1.543$$

And β_3 and α_3 are =1, therefore; the exit loss coefficient, k_{exit} :

$$\begin{aligned} k_{exit} &= (2\beta_3 - \alpha_3) \left(\frac{Area_2}{Area_3} \right)^2 - 2\beta_2 \left(\frac{Area_2}{Area_3} \right) + \alpha_2 \\ &= (2(1) - 1) \left(\frac{0.020724}{0.025999} \right)^2 - 2(1.2) \left(\frac{0.020724}{0.025999} \right) + 1.543 = 0.26528 \end{aligned}$$

Now, Air Pressure Drop Across the Radiator, Δp :

$$\begin{aligned} \Delta p &= \left[k_{entrance} + f_{air} \frac{L_{air2}}{D_{h_{air2}}} + k_{exit} \right] \frac{\rho_{air} V_{air2}^2}{2} \\ \Delta p &= \left(\left[0.80 + 0.13652 \frac{0.2403m}{0.001643m} + 0.26528 \right] \right) \left(\frac{(1.21 \frac{kg}{m^3})(5.1072^2 \frac{m}{s})}{2} \right) = 64.98 Pa \end{aligned}$$

Note that this calculated value of air pressure drop is at an air velocity of $5.1072^2 \frac{m}{s}$, and the velocity of air will not always be at this value however, it will change once the car is in motion causing more air flow through the radiator fins which results in better cooling.

A generated plot is shown below, **Figure 18**, which gives a better idea of how pressure drop is affected by the air velocity when the car is motion and speeding up.

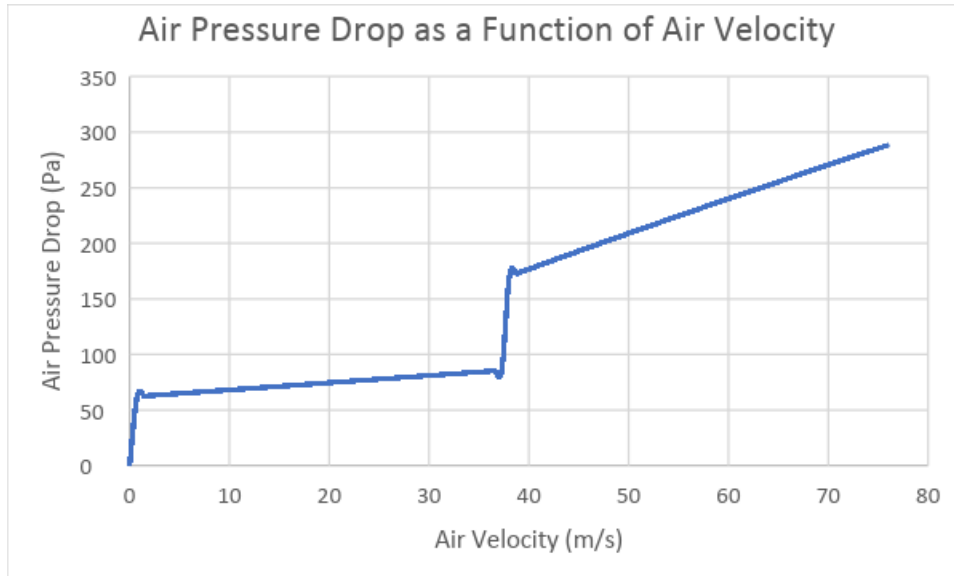


Figure 18: *Air pressure drop as a function of air velocity*

Note, the straight vertical line can reach up to 38 m/s. That causes air flow changing from laminar to turbulent and therefore affecting the pressure drop. Therefore, the air pressure drop increases as the air velocity increases.

Pump

To ensure the greatest amount of suction provided by the pump, it must be placed at the lowest spot in the system. The cooling system is required to cool the motor and the inverter. The motor will get hotter and has a lower temperature sensitivity than the inverter. This means the motor must be placed before the inverter in the cooling loop. The pump is placed between the radiator and the motor so that it pulls the cooled water from the radiator and supplies it to the pump.

In the same fashion as in determining air pressure drop, the water pressure drop also depends on multiple factors. The most important factor is the water flow rate through the radiator tubes. This is determined by the speed of the pump. Another important factor is the geometry of the radiator tubes as well as the material of which it is made of. Another big factor in calculating the water pressure drop are the loss coefficients of the entrance and exit which are controlled by the model of our radiator. **Figure 19** below shows the flow of water across the radiator tubes. Sections 0 and 1 show the water entering and exiting the radiator, respectively.

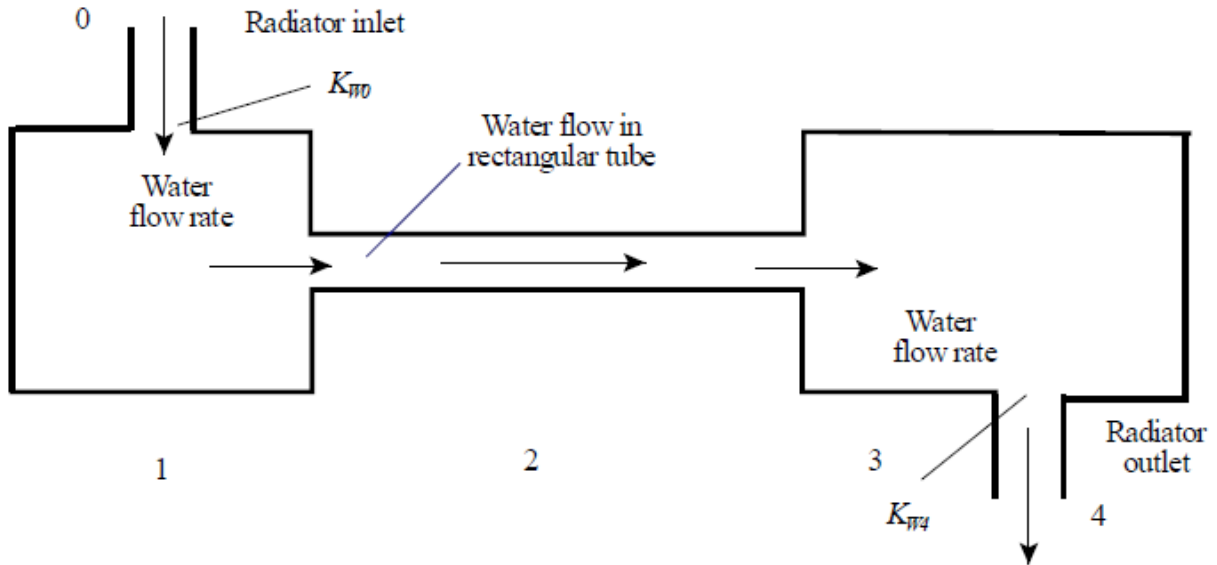


Figure 19: Demonstrative model of water flow in the radiator

Before determining the pressure drop, geometry calculations of rectangular water tubes must be conducted as shown below.

Flow area of the rectangular water tubes, $Area_{w2}$:

$$Area_{w2} = \text{number of tubes} * \text{tube width} * \text{inside length} = 0.00060695 \text{ m}^2$$

Outlet area of water pipe, $Area_{w4}$:

$$Area_{w4} = \frac{\pi}{4} * \text{diameter}^2 = 0.00022746 \text{ m}^2$$

Area ratios

$$\frac{Area_{w2}}{Area_{w4}} = \frac{0.00060695 \text{ m}^2}{0.00022746 \text{ m}^2} = 2.66836$$

$$\frac{Area_{w2}}{Area_{w1}} = \frac{Area_{w2}}{Area_{w3}} = \frac{20 (0.001559\text{m})}{0.24028\text{m}} = 0.12976$$

Where $Area_{w1} = Area_{w3}$, are the upstream and downstream flow areas of water tubes, respectively.

Since the radiator has rectangular water tubes, the hydraulic diameter should be used.

The hydraulic diameter of water tubes, D_{hw2} :

$$D_{hw2} = \frac{4(\text{flow area})}{\text{perimeter}} = \frac{4(0.019466 * 0.001559)}{2(0.019466 + 0.001559)} = 0.0028868 \text{ m}$$

Average water tube velocity, V_2 :

$$V_2 = \frac{\left(\frac{12 \text{ L}}{\text{min}}\right) \left(\frac{1 \text{ m}^3}{1000 \text{ L}}\right) \left(\frac{\text{min}}{60 \text{ sec}}\right)}{20(1.559 \text{ mm})(19.466 \text{ mm})} = 0.32952 \frac{\text{m}}{\text{s}}$$

Ratio of relative roughness, ε , of Aluminum to the hydraulic diameter, D_{hw2} :

$$\frac{\varepsilon}{D_{hw2}} = \frac{0.0000015 \text{ m}}{0.0028868 \text{ m}} = 0.0005196$$

The Reynolds number,

$$Re_{w2} = \frac{\text{velocity} * \text{hydraulic diameter}}{\text{kinematic viscosity of water}} = \frac{V_2 D_{hw2}}{\nu_2} = \frac{(0.32952 \frac{\text{m}}{\text{s}})(0.0028868 \text{ m})}{3 \times 10^{-7} \frac{\text{m}^2}{\text{s}}} = 3170.8$$

Note that Reynolds number is greater than 2300, therefore; the flow is turbulent.

The friction factor in the water tube, f_{w2} :

$$f_{w2} = \frac{1.325}{\left[\ln \ln \left(\frac{\varepsilon}{3.7 D_{hw2}} + \frac{5.74}{Re_{hw2}^{0.9}} \right) \right]^2} = \frac{1.325}{\left[\ln \ln \left(\frac{0.0005196}{3.7} + \frac{5.74}{3170.8^{0.9}} \right) \right]^2} = 0.0442178$$

Water tube entrance loss coefficient, $K_{entrance}$:

$$K_{entrance} = K_L \left(1 - \frac{\text{Area}_{w2}}{\text{Area}_{w1}} \right) = 0.42 (1 - 0.12976) = 0.3659$$

Where K_L is obtained from Appendix A. Also, note that the loss coefficient for a sudden contraction is a function of the area ratio, $\frac{\text{Area}_1}{\text{Area}_2}$.

Water tube exit loss coefficient, K_{exit} :

$$K_{exit} = \left(1 - \frac{Area_{w2}}{Area_{w3}}\right)^2 = (1 - 0.12976)^2 = 0.75731$$

The density of water, ρ_w , = $1000 \frac{kg}{m^3}$, and the length of the water tube, L_{w2} , is $0.2403m$. Additionally; $k_{wo} = 1$ for sharp edged exit flow; see **Figure App.A.4**. And $k_{w4} = 0.5$ for sharp edged entrance flow; check **Figure App.A.3** in the Appendix A section of this report.

With all the calculated and know variables, the water pressure drop across the radiator can be calculated as follows.

Water Pressure Drop Across the Radiator

$$\Delta p = \left[k_{enterance} + f_{w2} \frac{L_{w2}}{D_{hw2}} + k_{exit} \right] \frac{\rho_w V_{w2}^2}{2} + [k_{wo} + k_{w4}] \frac{\rho_w V_{wo}^2}{2}$$

$$\Delta p = \left(\left[0.3659 + 0.0442 \frac{0.2403m}{0.002999m} + 0.75731 \right] + [(1 + 0.5)(2.668)^2] \right) \left(\frac{(1000 \frac{kg}{m^3})(0.32952^2 \frac{m}{s})}{2} \right) = 840.6 Pa$$

This value of water pressure drop, $840.6 Pa$, is generated at a specific water velocity of $0.32952^2 \frac{m}{s}$, however, this is not always the case. Depending on the operating pump speed which has a maximum flow rate of 12 lpm, the volumetric flow rate of water changes and therefore changing the velocity. A graph representation is a better choice to express the water pressure drop for various volumetric flow rates. **Figure 20** shows water pressure drop as a function of volumetric flow rate. Note, the pressure drop increases as the volumetric rate increases.

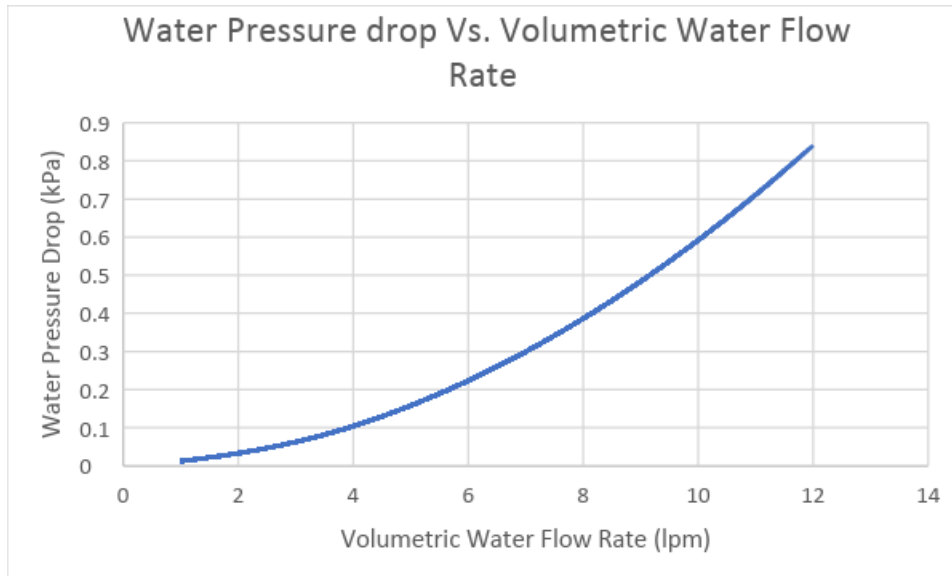


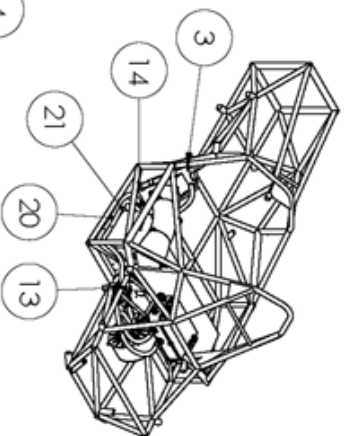
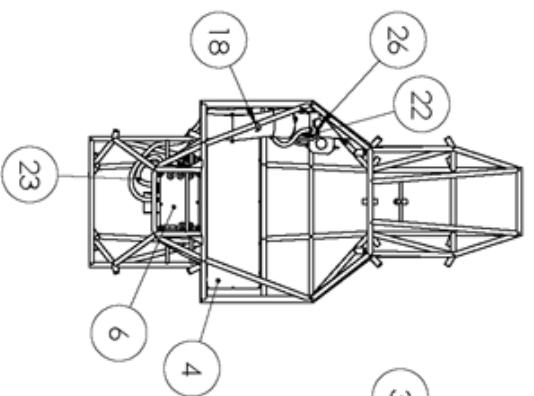
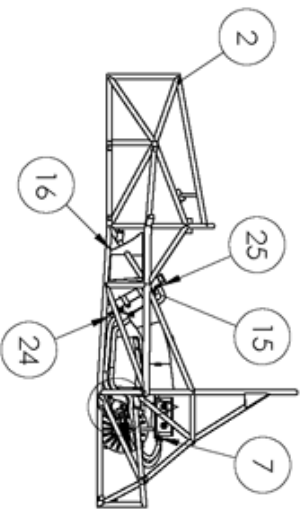
Figure 20: *Water pressure drop as a function of volumetric flow rate*

The motor and the inverter also contributed significantly to the total water pressure drop created by the system. The motor and the inverter have factory rated pressure drops of 90 kPa and 30 kPa, respectively. Adding these pressure drops to the one calculated for the radiator gives a total water pressure drop of 120.84 kPa, with the pressure drop developed through tubes being negligible. This allowed us to determine the size of pump need. As long as the pump provides a head pressure large enough to overcome the systems pressure drop, it will work fine. on the electrical side of things, the water pump can not exceed 12V, as it is wired into the low voltage circuit of the car.

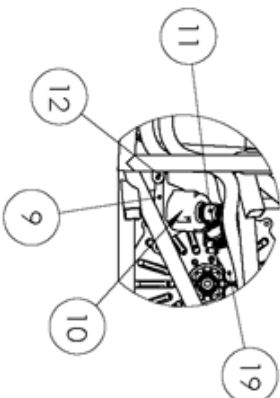
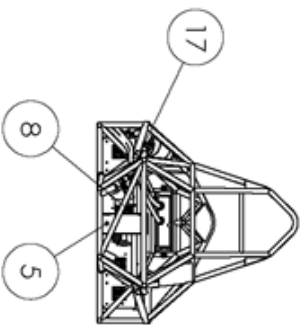
We choose the Davies Craig EBP40 electric booster pump. This pump supplies enough head pressure to overcome the total pressure drop through the system at a decent flow rate. Mounting tabs for the pump were laser cut and welded to the frame (drawing in Appendix E). the pump required a straight fitting reducer and straight male to male barb to connect to the water tubing since its ID is $\frac{5}{8}$ " and the outlet of the pump is $\frac{3}{4}$ ".

Figure 21 below is a drawing of the overall cooling system assembly within the frame of the car. Included in the drawing is the bill of materials with everything included and the locations and connections between the motor and inverter.

ITEM NO.	PART NUMBER	DESCRIPTION	QTY.
1	SKELETON	ZER-19 Frame rev-2	1
2	W703-18	RADIATOR ASSEMBLY	1
3	S802	MOTOR	1
4	Accumulator	INVERTER	1
5	EMRAX 228		1
6	RMS PM100		1
7	Inverter Fitting A16-0.625 Barb		2
8	Motor Coolant Fitting 0.625 Barb		2
9	PUMP MOUNT		1
10	P802-00	WATER PUMP	1
11	P812-00	0.75x0.625 STRAIGHT REDUCER	2
12	M813-00	PUMP MOUNTING TAB	2
13	0.625 MALE TO MALE BARB		3
14	M809-00	LOWER RADIATOR MOUNTING TAB	1
15	M808-00	UPPER RADIATOR MOUNTING TAB	1
16	M810-00	INLET MOUNTING TAB	2
17	M811-00	EXHAUST MOUNTING TAB	2
18	M812-00	MIDDLE DUCT TAB	1
19	PUMP TO MOTOR		1
20	RADIATOR TO PUMP		1
21	CONTROLLER TO RADIATOR		1
22	RAD TO CATCHCAN		1
23	MOTOR TO CONTROLLER		1
24	0.625 ANGLE FITTING		1
25	HOSE CLAMP		14
26	SMALL HOSE CLAMP		2



DETAIL A
SCALE 1:9



ZIPS ELECTRIC RACING THE UNIVERSITY OF AKRON		TOLERANCES		ENGINEERING APPROVAL:	
FRACTION ±1/16		DECIMAL		DATE:	
X ±0.00		XXX ±0.03		SCALE: 1:50	
MODEL/NAME		DESCRIPTION		SHEET:	
502 E BUCHTEL AVE, AKRON, OH, 44325		Cooling System		-PART DESCRIPTION-	

Figure 21: Cooling System Assembly

Budget

Throughout the course of the year, we learned a lot about the specific workings of our subsystem. With some trial and error, it became apparent what would work and what would not. Due to this, certain items on our purchase request form inevitably needed to be returned as we pivoted and developed new strategies and approaches for the subsystem design. Resulting from this, our original anticipated budget amount gradually changing throughout both semesters. One major example in a significant budget shift was the decision not to incorporate the proposed experiment to model the cooling system separate from the car in order to empirically determine cooling load. Therefore, any and all items bought for the experiment were no longer needed and will be returned. As illustrated in **Figure App.D.1**, our original budget amounted to just over \$900 which was within the realm of what we were expecting. As denoted in the same figure, we highlighted item part numbers to be returned in red.

Chapter 5: Discussion

Designing and analyzing the cooling system for the Zips Formula Electric car was a great senior design project that exposed our group to the real life applications design team work of being an engineer. The work done for this project is essentially translatable to the automotive and HVAC industries. Fundamental laws and concepts had to be applied in order to complete this project successfully. Some of which include the law of thermodynamics and Bernoulli's conservation of energy principle. Although it was challenging to know where to begin since the Zips Formula Electric Race Car team had no cooling subsystem team before, now there is a solid foundation for the cooling teams to come to build upon. Appendix G of this report has an experimental proposal for the next year's cooling team to perform and calculate the cooling load through experimentation.

Chapter 6: Conclusion

The four years of learning about what goes into becoming an engineering concludes with apply the knowledge in a senior design project. In successfully completing this project, we used principles learned in Thermodynamics, Heat Transfer, Fluid Mechanics and Concepts of Design. We were also able to create design which performed a specific task in accordance to Formula Electric guidelines and design choices made for the team as a whole.

Next year's cars

The design, calculations and general knowledge can be used by next year's Formula Electric car team to build on. We wanted to leave next year's team with recommendations for

things to add that would improve the car even further. Some of these include a thermometer of the water in the system. Right now we can only see a readout of the max inverter and motor temperature when a computer is attached. It would be beneficial to track this more thoroughly with a thermometer in real-time while the car is operating. This coupled with a water flow meter would improve the cooling system further. Ultimately the cooling system pump or fan can be automated to turn on or off according to the temperature of the coolant. This is the same way a car thermostat works. This helps insure that the inverter and motor stay at their appropriate temperature. Additionally, Included in Appendix F is a layout of a suggested experiment which could be performed by the team next year.

References

- [1] Lienhard IV, John H. Lienhard V, John H. *A Heat Transfer Textbook*. 4th edition. 2017.
- [2] Munson, Bruce R. Okiishi, Theodore H. Huebsch, Wade H. Rothmayer, Alric P.
Fundamentals of Fluid Mechanics, 7th edition. 2013.
- [3] Gross, Richard J. *Vehicle Dynamics*. Chapter 11: Cooling System Design. 2015.

Appendices

Appendix A:

Viscous Flow Loss Coefficients

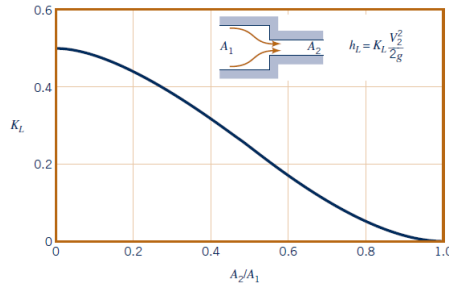








Figure 8.26
Loss coefficient for a sudden contraction (Ref. 10).

Figure App.A.1: Loss coefficient for a sudden contraction. [ref 2]

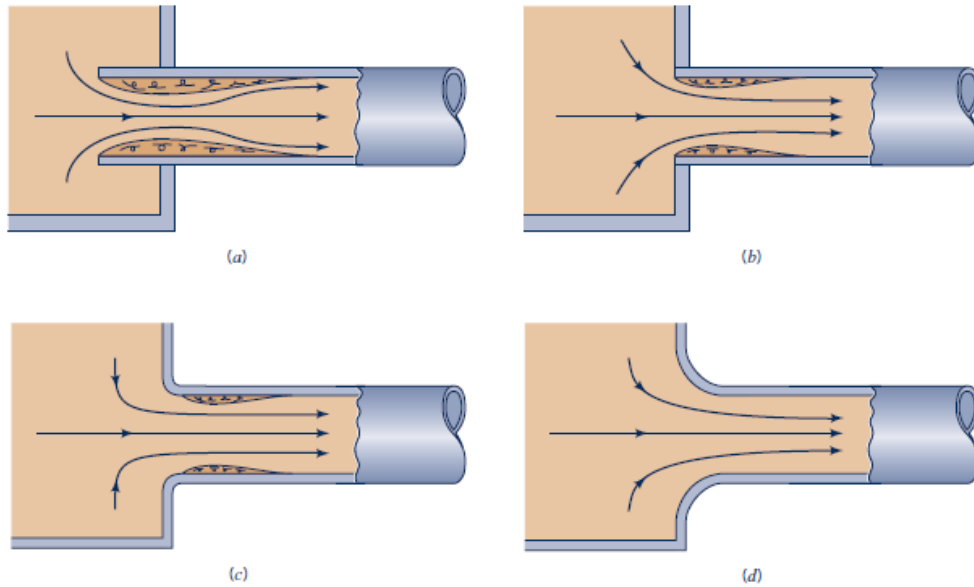
Table 8.2

Loss Coefficients for Pipe Components ($h_L = K_L \frac{V^2}{2g}$) (Data from Refs. 5, 10, 27)

Component	K_L	
a. Elbows		
Regular 90°, flanged	0.3	 90° elbow
Regular 90°, threaded	1.5	
Long radius 90°, flanged	0.2	
Long radius 90°, threaded	0.7	
Long radius 45°, flanged	0.2	
Regular 45°, threaded	0.4	
b. 180° return bends		
180° return bend, flanged	0.2	 45° elbow
180° return bend, threaded	1.5	
c. Tees		
Line flow, flanged	0.2	 180° return bend
Line flow, threaded	0.9	
Branch flow, flanged	1.0	
Branch flow, threaded	2.0	
d. Union, threaded		
	0.08	 Tee
e. Valves		
Globe, fully open	10	 Tee
Angle, fully open	2	
Gate, fully open	0.15	
Gate, $\frac{1}{2}$ closed	0.26	
Gate, $\frac{3}{4}$ closed	2.1	
Gate, $\frac{1}{2}$ closed	17	 Union
Swing check, forward flow	2	
Swing check, backward flow	∞	
Ball valve, fully open	0.05	
Ball valve, $\frac{1}{2}$ closed	5.5	
Ball valve, $\frac{3}{4}$ closed	210	

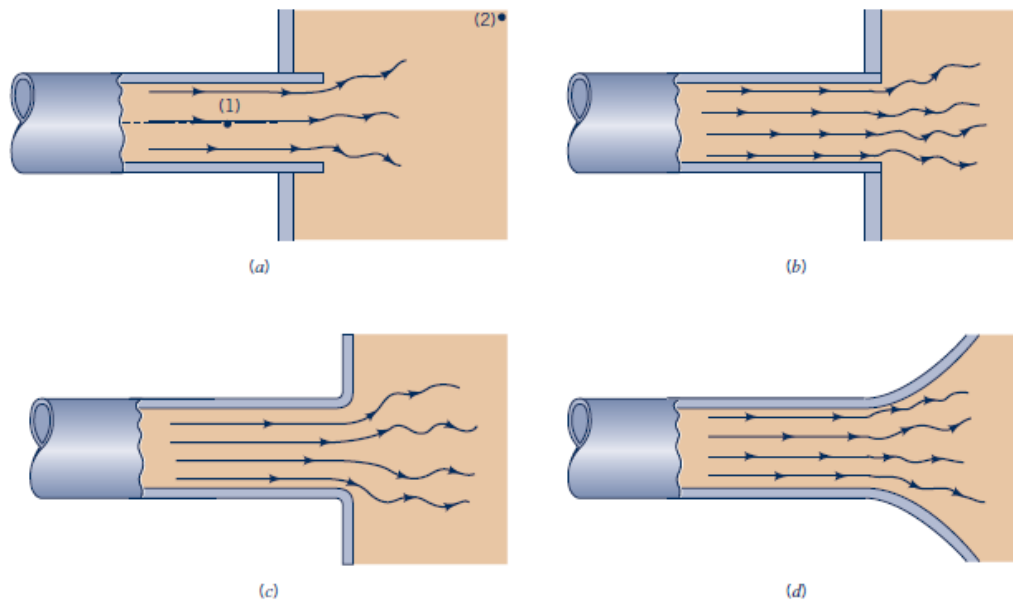
*See Fig. 8.32 for typical valve geometry.

Figure App.A.2: Loss coefficients for different pipe orientation. [ref 2]



■ **Figure 8.22** Entrance flow conditions and loss coefficient (Data from Refs. 28, 29).
 (a) Reentrant, $K_L = 0.8$, (b) sharp-edged, $K_L = 0.5$, (c) slightly rounded, $K_L = 0.2$ (see Fig. 8.24),
 (d) well-rounded, $K_L = 0.04$ (see Fig. 8.24).

Figure App.A.3: Entrance flow conditions and loss coefficient. [ref 2]



■ **Figure 8.25** Exit flow conditions and loss coefficient.
 (a) Reentrant, $K_L = 1.0$, (b) sharp-edged, $K_L = 1.0$, (c) slightly rounded, $K_L = 1.0$,
 (d) well-rounded, $K_L = 1.0$.

Figure App.A.4: Exit flow conditions and loss coefficient. [ref 2]

Appendix B:

Thermal Properties of Fluids and Metals

<i>Temperature</i>								
K	°C	ρ (kg/m ³)	c_p (J/kg·K)	k (W/m·K)	α (m ² /s)	ν (m ² /s)	Pr	β (K ⁻¹)
Water								
273.16	0.01	999.8	4220	0.5610	1.330×10^{-7}	17.91×10^{-7}	13.47	-6.80×10^{-5}
275	2	999.9	4214	0.5645	1.340	16.82	12.55	-3.55×10^{-5}
280	7	999.9	4201	0.5740	1.366	14.34	10.63	4.36×10^{-5}
285	12	999.5	4193	0.5835	1.392	12.40	8.91	0.000112
290	17	998.8	4187	0.5927	1.417	10.85	7.66	0.000172
295	22	997.8	4183	0.6017	1.442	9.600	6.66	0.000226
300	27	996.5	4181	0.6103	1.465	8.568	5.85	0.000275
305	32	995.0	4180	0.6184	1.487	7.708	5.18	0.000319
310	37	993.3	4179	0.6260	1.508	6.982	4.63	0.000361
320	47	989.3	4181	0.6396	1.546	5.832	3.77	0.000436
340	67	979.5	4189	0.6605	1.610	4.308	2.68	0.000565
360	87	967.4	4202	0.6737	1.657	3.371	2.03	0.000679
373.15	100.0	958.3	4216	0.6791	1.681	2.940	1.75	0.000751
400	127	937.5	4256	0.6836	1.713	2.332	1.36	0.000895
420	147	919.9	4299	0.6825	1.726	2.030	1.18	0.001008
440	167	900.5	4357	0.6780	1.728	1.808	1.05	0.001132
460	187	879.5	4433	0.6702	1.719	1.641	0.955	0.001273
480	207	856.5	4533	0.6590	1.697	1.514	0.892	0.001440
500	227	831.3	4664	0.6439	1.660	1.416	0.853	0.001645
520	247	803.6	4838	0.6246	1.607	1.339	0.833	0.001909
540	267	772.8	5077	0.6001	1.530	1.278	0.835	0.002266
560	287	738.0	5423	0.5701	1.425	1.231	0.864	0.002783
580	307	697.6	5969	0.5346	1.284	1.195	0.931	0.003607
600	327	649.4	6953	0.4953	1.097	1.166	1.06	0.005141
620	347	586.9	9354	0.4541	0.8272	1.146	1.39	0.009092
640	367	481.5	25,940	0.4149	0.3322	1.148	3.46	0.03971
642	369	463.7	34,930	0.4180	0.2581	1.151	4.46	0.05679
644	371	440.7	58,910	0.4357	0.1678	1.156	6.89	0.1030
646	373	403.0	204,600	0.5280	0.06404	1.192	18.6	0.3952
647.0	374	357.3	3,905,000	1.323	0.00948	1.313	138.	7.735

Figure App.B.1: Thermal properties of water at different temperatures. [ref 1]

Metal	Properties at 20°C				Thermal Conductivity, k (W/m·K)									
	ρ (kg/m ³)	c_p (J/kg·K)	k (W/m·K)	α (10 ⁻⁵ m ² /s)	-170°C	-100°C	0°C	100°C	200°C	300°C	400°C	600°C	800°C	1000°C
Aluminums														
Pure	2,707	905	237	9.61	302	242	236	240	238	234	228	215	≈95 (liq.)	
99% pure			211		220	206	209							
Duralumin (≈4% Cu, 0.5% Mg)	2,787	883	164	6.66		126	164	182	194					
Alloy 6061-T6	2,700	896	167	6.90			166	172	177	180				
Alloy 7075-T6	2,800	841	130	5.52	76	100	121	137	172	177				
Chromium	7,190	453	90	2.77	158	120	95	88	85	82	77	69	64	62
Cupreous metals														
Pure Copper	8,954	384	398	11.57	483	420	401	391	389	384	378	366	352	336
DS-C15715*	8,900	≈384	365	≈10.7			367	355	345	335	320			
Beryllium copper (2.2% Be)	8,250	420	103	2.97				117						
Brass (30% Zn)	8,522	385	109	3.32	73	89	106	133	143	146	147			
Bronze (25% Sn) [§]	8,666	343	26	0.86										
Constantan (40% Ni)	8,922	410	22	0.61	17	19	22	26	35					
German silver (15% Ni, 22% Zn)	8,618	394	25	0.73	18	19	24	31	40	45	48			
Gold	19,320	129	318	12.76	327	324	319	313	306	299	293	279	264	249
Ferrous metals														
Pure iron	7,897	447	80	2.26	132	98	84	72	63	56	50	39	30	29.5
Cast iron (4% C)	7,272	420	52	1.70										
Steels (C ≤ 1.5%)														
AISI 1010 ^{††}	7,830	434	64	1.88		70	65	61	55	50	45	36	29	
0.5% carbon	7,833	465	54	1.47			55	52	48	45	42	35	31	29
1.0% carbon	7,801	473	43	1.17			43	43	42	40	36	33	29	28
1.5% carbon	7,753	486	36	0.97			36	36	36	35	33	31	28	28

Figure App.B.2: Thermal properties of different metals at different temperatures. [ref 1]

T (K)	ρ (kg/m ³)	c_p (J/kg·K)	μ (kg/m·s)	ν (m ² /s)	k (W/m·K)	α (m ² /s)	Pr
Air							
100	3.605	1039	0.711×10^{-5}	0.197×10^{-5}	0.00941	0.251×10^{-5}	0.784
150	2.368	1012	1.035	0.437	0.01406	0.587	0.745
200	1.769	1007	1.333	0.754	0.01836	1.031	0.731
250	1.412	1006	1.606	1.137	0.02241	1.578	0.721
260	1.358	1006	1.649	1.214	0.02329	1.705	0.712
270	1.308	1006	1.699	1.299	0.02400	1.824	0.712
280	1.261	1006	1.747	1.385	0.02473	1.879	0.711
290	1.217	1006	1.795	1.475	0.02544	2.078	0.710
300	1.177	1007	1.857	1.578	0.02623	2.213	0.713
310	1.139	1007	1.889	1.659	0.02684	2.340	0.709
320	1.103	1008	1.935	1.754	0.02753	2.476	0.708
330	1.070	1008	1.981	1.851	0.02821	2.616	0.708
340	1.038	1009	2.025	1.951	0.02888	2.821	0.707
350	1.008	1009	2.090	2.073	0.02984	2.931	0.707
400	0.8821	1014	2.310	2.619	0.03328	3.721	0.704
450	0.7840	1021	2.517	3.210	0.03656	4.567	0.703
500	0.7056	1030	2.713	3.845	0.03971	5.464	0.704
550	0.6414	1040	2.902	4.524	0.04277	6.412	0.706
600	0.5880	1051	3.082	5.242	0.04573	7.400	0.708
650	0.5427	1063	3.257	6.001	0.04863	8.430	0.712
700	0.5040	1075	3.425	6.796	0.05146	9.498	0.715
750	0.4704	1087	3.588	7.623	0.05425	10.61	0.719
800	0.4410	1099	3.747	8.497	0.05699	11.76	0.723
850	0.4150	1110	3.901	9.400	0.05969	12.96	0.725
900	0.3920	1121	4.052	10.34	0.06237	14.19	0.728
950	0.3716	1131	4.199	11.30	0.06501	15.47	0.731
1000	0.3528	1142	4.343	12.31	0.06763	16.79	0.733
1100	0.3207	1159	4.622	14.41	0.07281	19.59	0.736
1200	0.2940	1175	4.891	16.64	0.07792	22.56	0.738
1300	0.2714	1189	5.151	18.98	0.08297	25.71	0.738
1400	0.2520	1201	5.403	21.44	0.08798	29.05	0.738
1500	0.2352	1211	5.648	23.99	0.09296	32.64	0.735

Figure App.B.3: Thermal properties of air at different temperatures. [ref 1]

Appendix C

Provided by Manufacturers

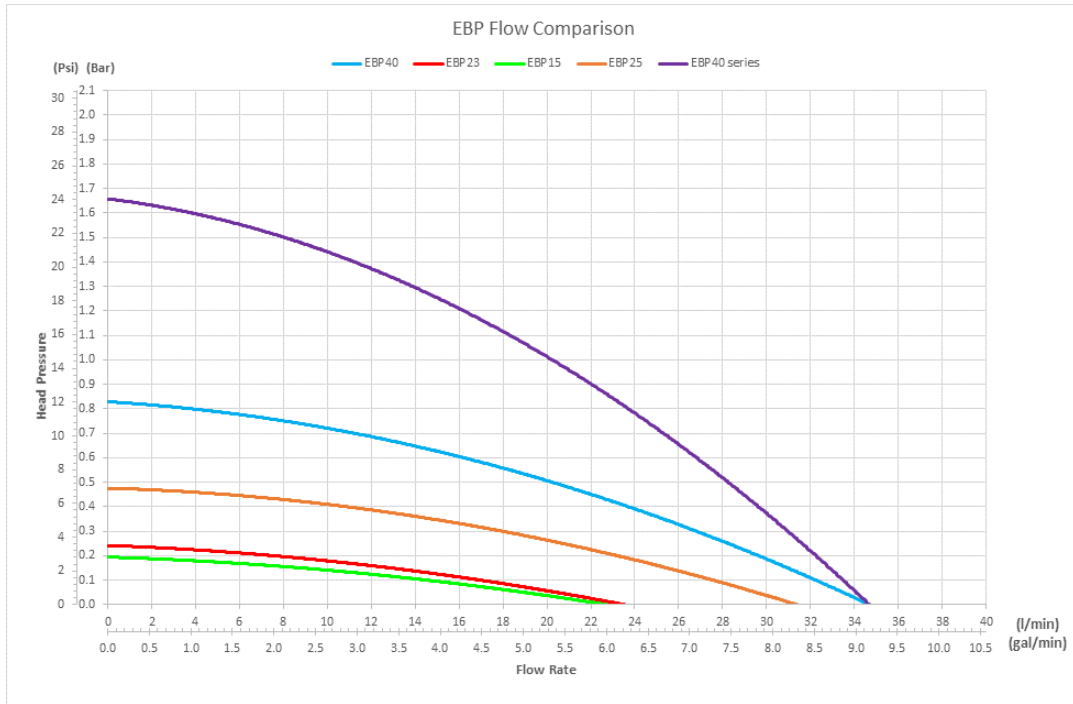


Figure App.C.1: Pump performance curve

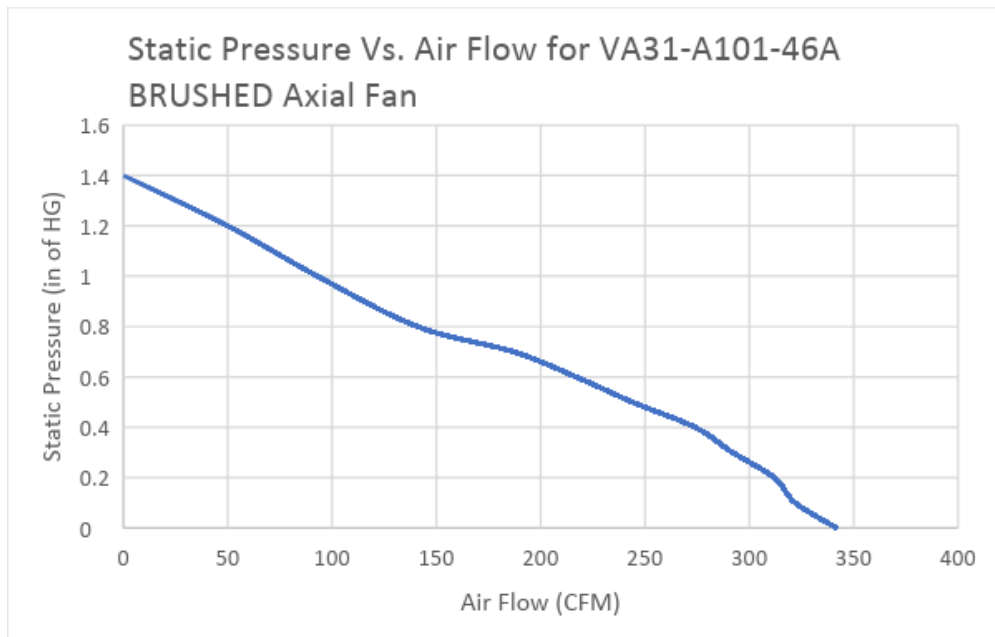


Figure App.C.2: Fan performance curve

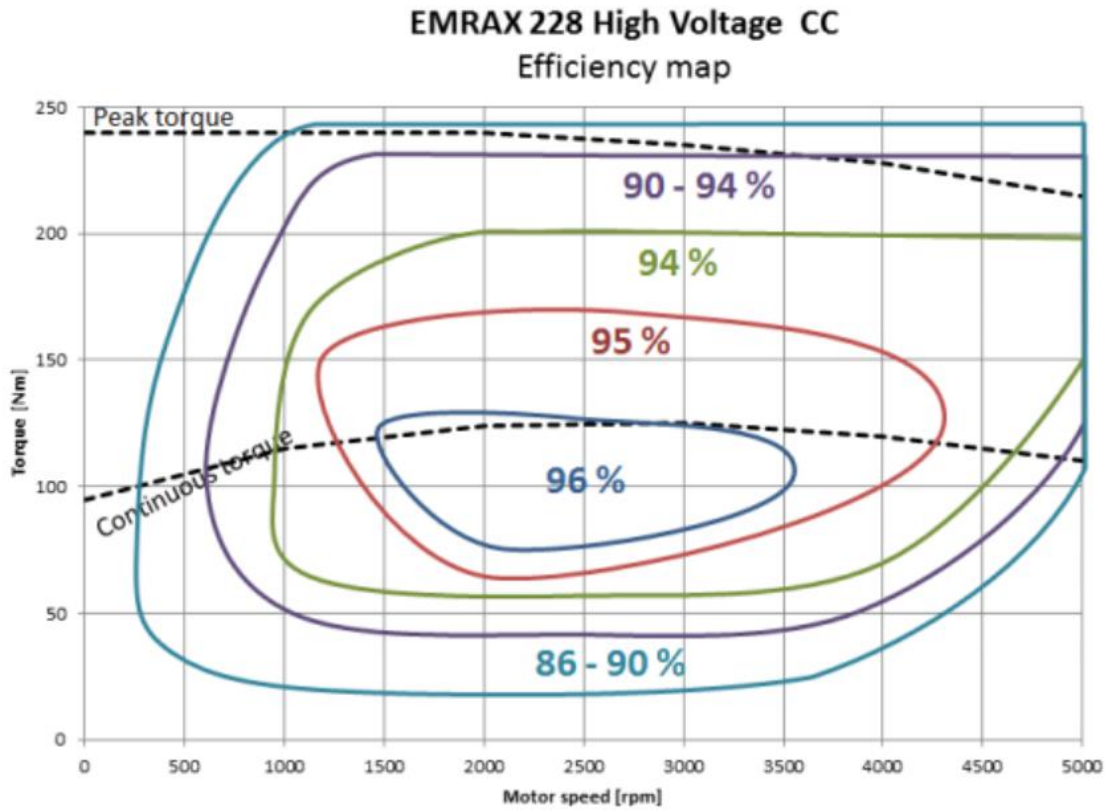


Figure App.C.3: Motor efficiency map

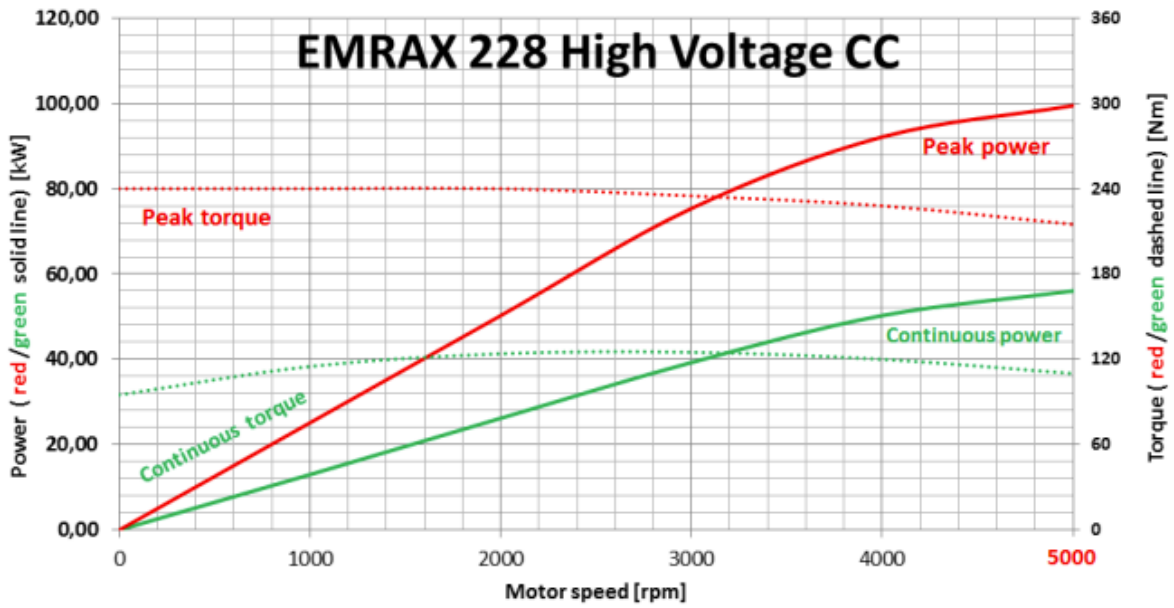


Figure App.C.3: Peak/continuous power and torque curves as function of engine speed

Appendix D:

Finances

Part Number	Item Description	Supplier	Cost/unit	Quantity	Total Cost	Date Requested
30103011	Spal Paddle Blade Low-Profile Electric Fans	Summit Racing	\$ 59.67	1	\$ 59.67	12/22/2018
DC-9050	Davies Craig Electric Booster Pump Kits	Summit Racing	\$ 130.63	2	\$ 261.26	11/25/2018
5236K951	3/4" x 10 ft High-Temperature Silicone Rubber Tubing	McMaster-Carr	\$ 42.50	1	\$ 42.50	11/25/2018
31271	3/4" x 3/4" PVC Flexible Coupling	US Plastic Corp	\$ 8.62	2	\$ 17.24	11/25/2018
201-440	Thermocouple Type T 1/4" - 20 x 0.5" long	TC Direct	\$ 22.50	4	\$ 90.00	11/25/2018
PSLE-750M002	3/4 in. x 2 ft. Copper Type M Hard Straight Pipe	Home Depot	\$ 6.21	1	\$ 6.21	11/25/2018
PP1	1in. x 2 ft. x 2ft. Foam Insulation Board	HomeDepot	\$ 5.98	1	\$ 5.98	11/25/2018
6712595	1/2"-1 1/4" Hose Clamps	Home Depot	\$ 0.98	6	\$ 5.88	11/25/2018
EL12FT34	3/4" Easy Loc x 1/2" FPT Tee	DripWorks	\$ 5.95	1	\$ 5.95	11/25/2018
ELMT34	3/4" Easy Loc male hose tee	DripWorks	\$ 2.49	2	\$ 4.98	11/25/2018
HCAP	Hose Cap	DripWorks	\$ 0.35	2	\$ 0.70	11/25/2018
VAB12	Air Bleed - 1/2" MPT	DripWorks	\$ 4.95	2	\$ 9.90	11/25/2018
VAB34	Air Bleed - 3/4" MPT	DripWorks	\$ 9.95	2	\$ 19.90	11/25/2018
EL34F34	3/4" Easy Loc x 3/4" FPT	DripWorks	\$ 1.98	2	\$ 3.96	11/25/2018
AFHFP	Female Hose x 3/4" Female Pipe Fitting	DripWorks	\$ 1.95	2	\$ 3.90	11/25/2018
2500w	Immersion Water Heater	Walmart	\$ 10.99	2	\$ 21.98	11/25/2018
AS200U-75R	DAE Hot Water Meter	Amazon	\$ 40.99	1	\$ 40.99	11/25/2018
1487T5	UV-Resistant PVC Clear Tubing 3/4" ID, 1" OD 25ft	McMaster-Carr	\$ 60.00	1	\$ 60.00	1/22/2019
4429K137	90 Degree Elbow Reducer, 3/4 x 3/8 NPT Female	McMaster-Carr	\$ 14.32	2	\$ 28.64	1/22/2019
5350K45	Zinc-Plated Steel Barbed Hose Fitting 3/4" Hose ID, 3/4 NPT Male End	McMaster-Carr	\$ 4.06	2	\$ 8.12	1/22/2019
occ018-BK	Jegs Catch Can	JEGS	\$ 49.99	1	\$ 49.99	1/22/2019
8876T42	Nylon Plastic Loop Clamp	McMaster-Carr	\$ 14.69	1	\$ 14.69	1/22/2019
HM3-TY1LSH-B	Heinmo Catch Can	Amazon	\$ 39.99	1	\$ 39.99	4/4/2019
SR19.16	Silicone Straight Reducer 5/8 x 3/4	Pegasus Racing	\$ 9.39	2	\$ 18.78	4/7/2019
SR22.19	Silicone Straight Reducer 3/4 x 7/8	Pegasus Racing	\$ 9.69	2	\$ 19.38	3/19/2019
64326	5/8" Tube ID Black Nylon Coupler	US Plastic Corp	\$ 0.69	5	\$ 3.45	4/7/2019
61632	5/8" In-Line Hose Barb HFC 57 Series Polysulfone Coupling Body - Shutoff	US Plastic Corp	\$ 18.82	2	\$ 37.64	4/16/2019
61637	5/8" In-Line Hose Barb HFC 57 Series Polysulfone Coupling Insert - Shutoff	US Plastic Corp	\$ 13.18	2	\$ 26.36	4/16/2019
					\$ 908.04	

Figure App.D.1: Bill of materials

Appendix E

Solidworks Drawings

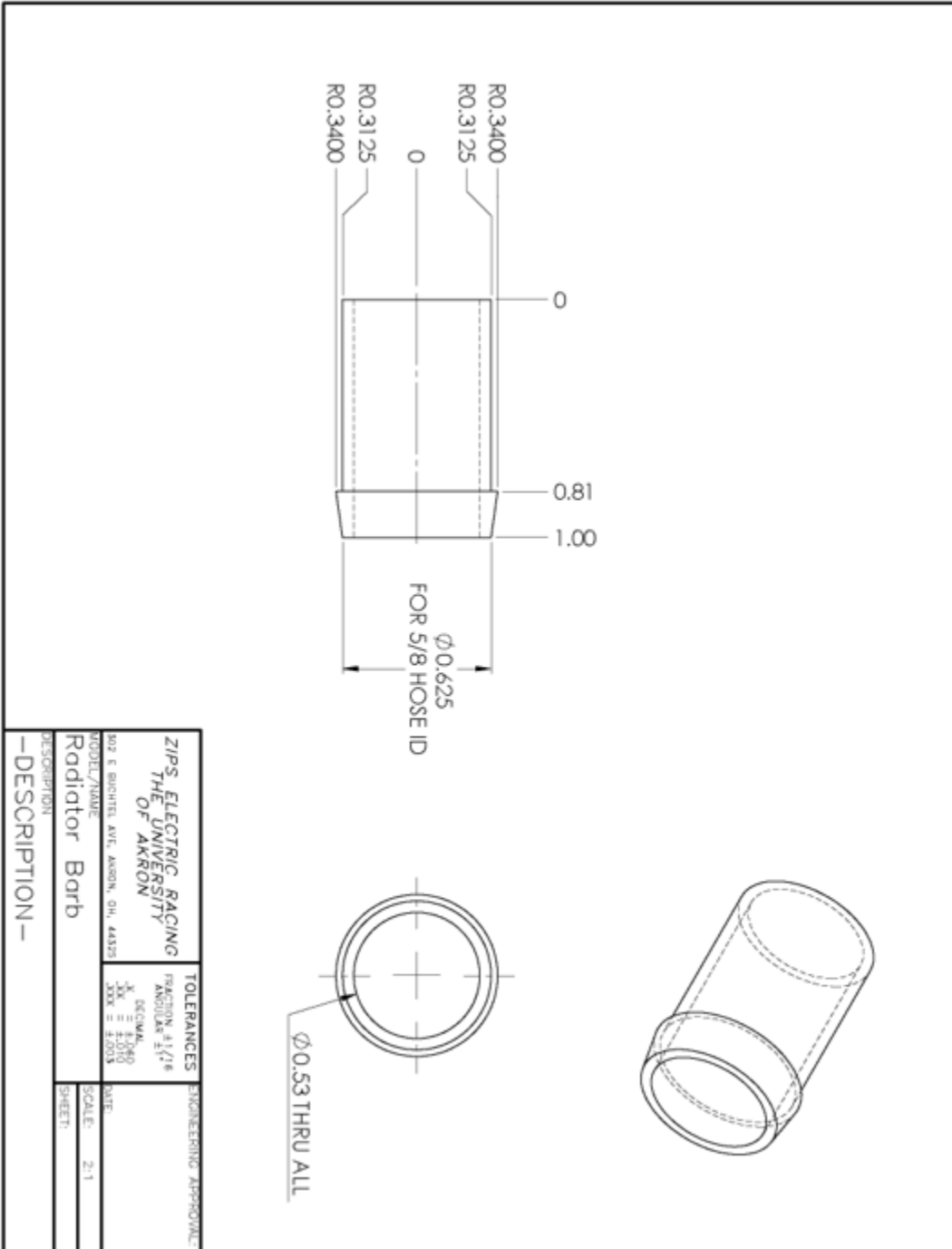
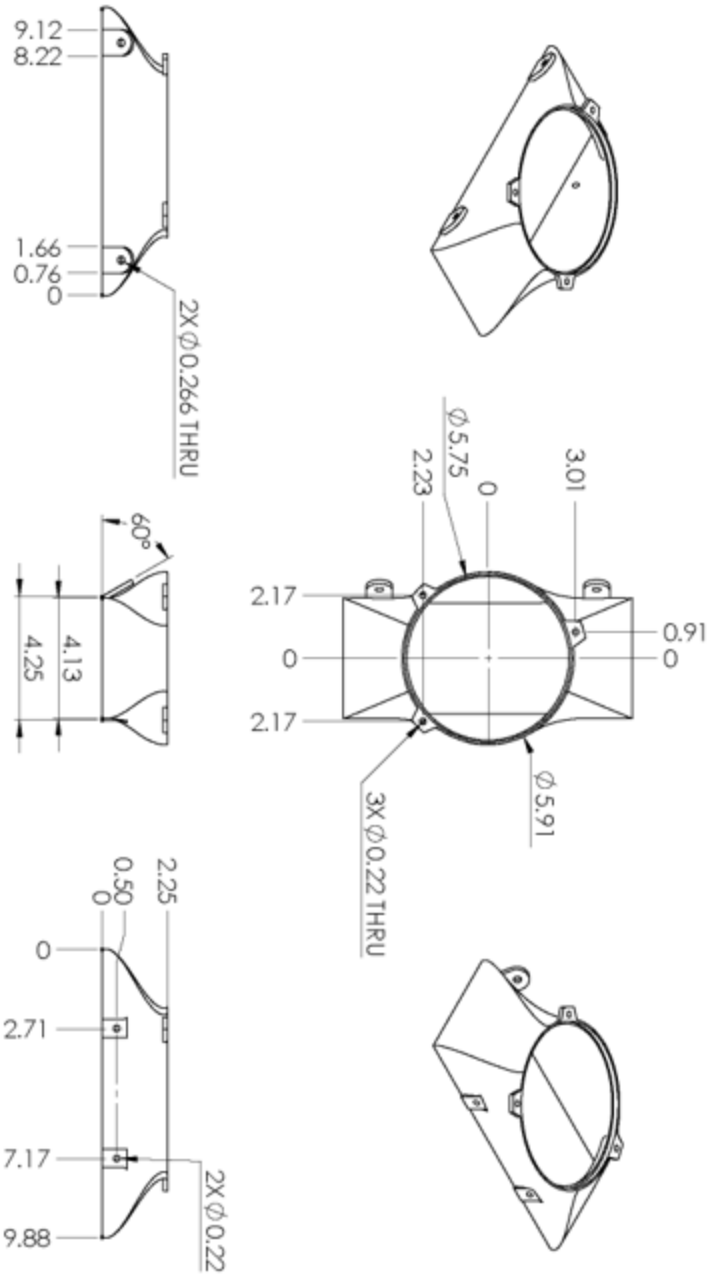


Figure App. E.1: Manufactured Radiator Barb to Replace the Old Ones



ZIPS ELECTRIC RACING THE UNIVERSITY OF AKRON		TOLERANCES FRACTION 1/16 ANGULAR 1/16 DECIMAL 1/16 ± 0.005 1/32 ± 0.003 1/64 ± 0.002		ENGINEERING APPROVAL DATE:	
302 E BRIGHT AVENUE, AKRON, OH, 44325		MODEL/ITERATION:		SCALE: 1:5	
RADIATOR TO FAN CONNECTION		DATE:		SHEET:	
DESCRIPTION —					

Figure App.E.2: 3D Printed Duct Piece that Connects the Fan to the Back Of the Radiator

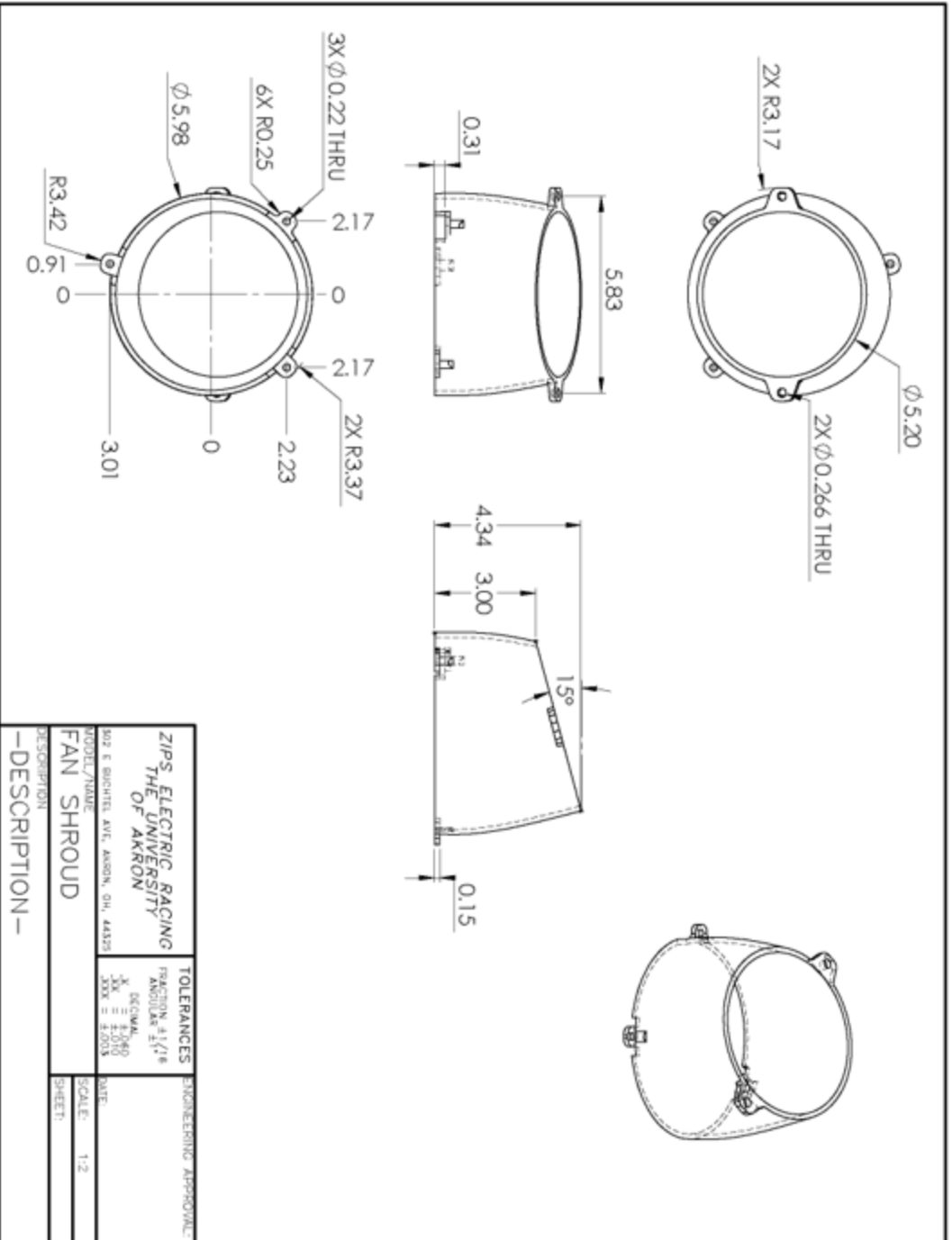


Figure App.E.3: 3D Printed Duct Piece that Shrouds the Fan

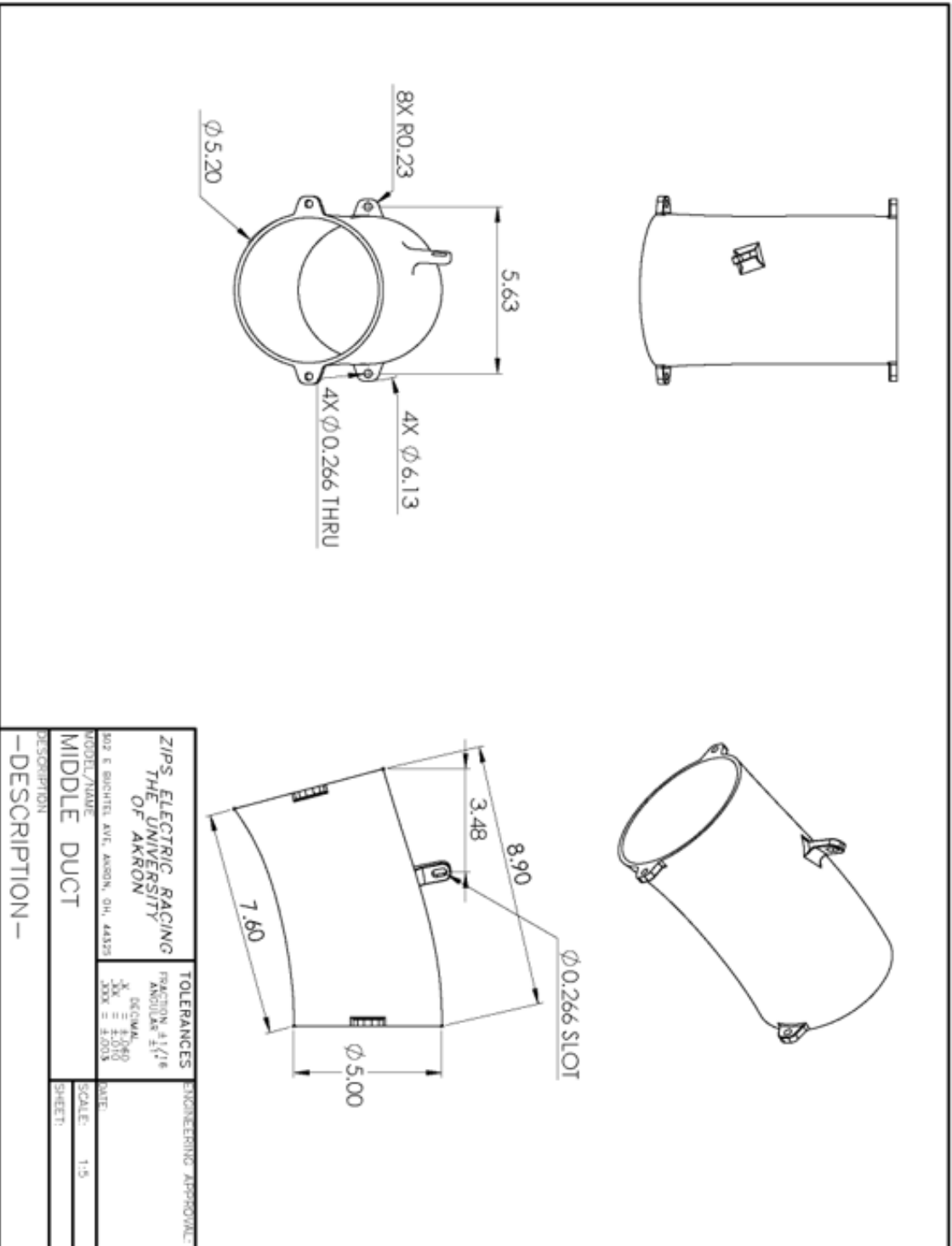


Figure App.E.4: 3D Printed Duct Piece that is Suspended Over the Accumulator

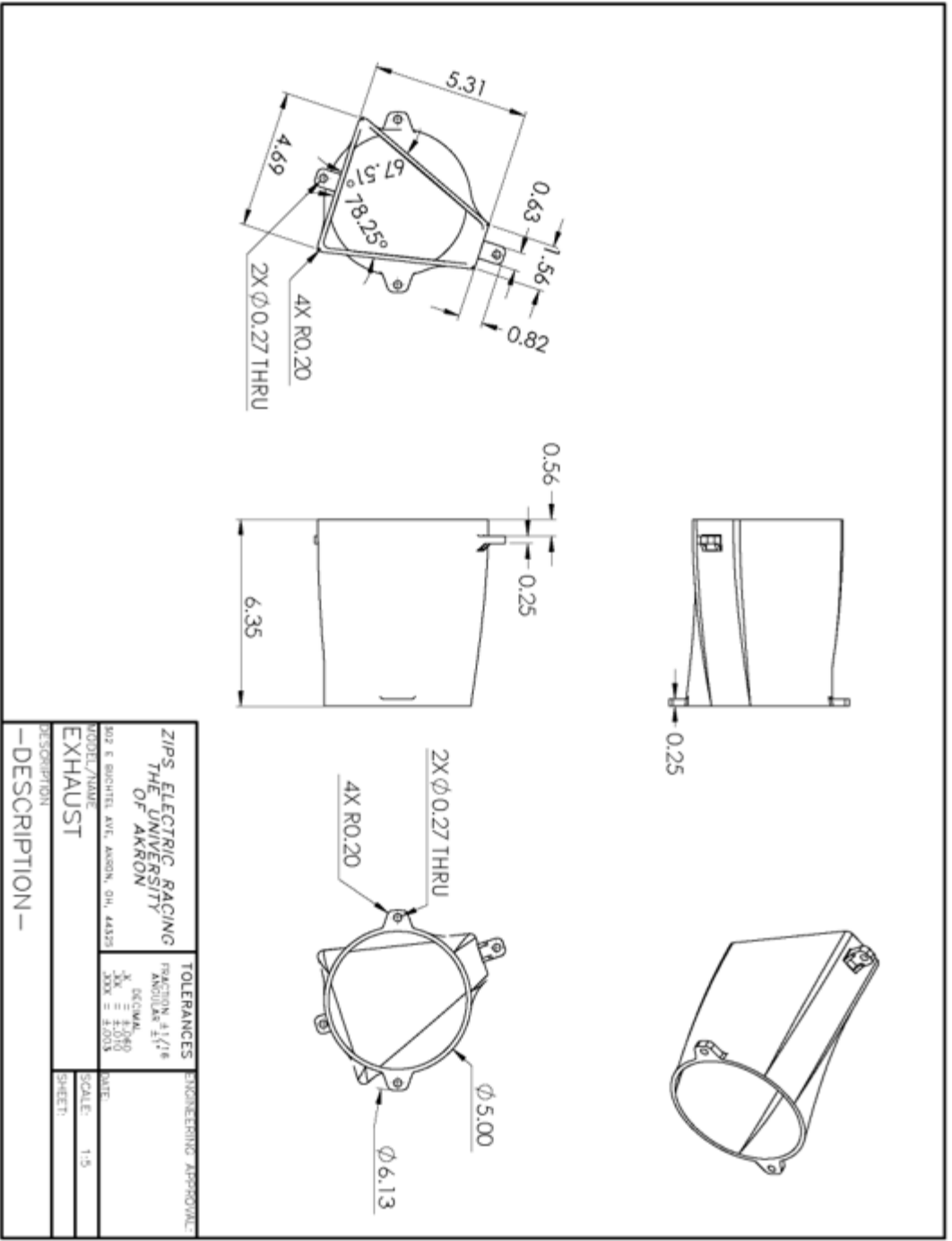


Figure App.E.5: 3D Printed Duct Piece which Vents Air Out of the Car

ZIPS ELECTRIC RACING THE UNIVERSITY OF AKRON		TOLERANCES FRACTION 1/16 DECIMAL ANGULAR 1/2°		ENGINEERING APPROVAL	
502 E BRIGHT AVENUE, AKRON, OH, 44325		DATE:		SCALE: 1:5	
MODEL/NAME EXHAUST		SHEET:		SHEET:	
DESCRIPTION —					

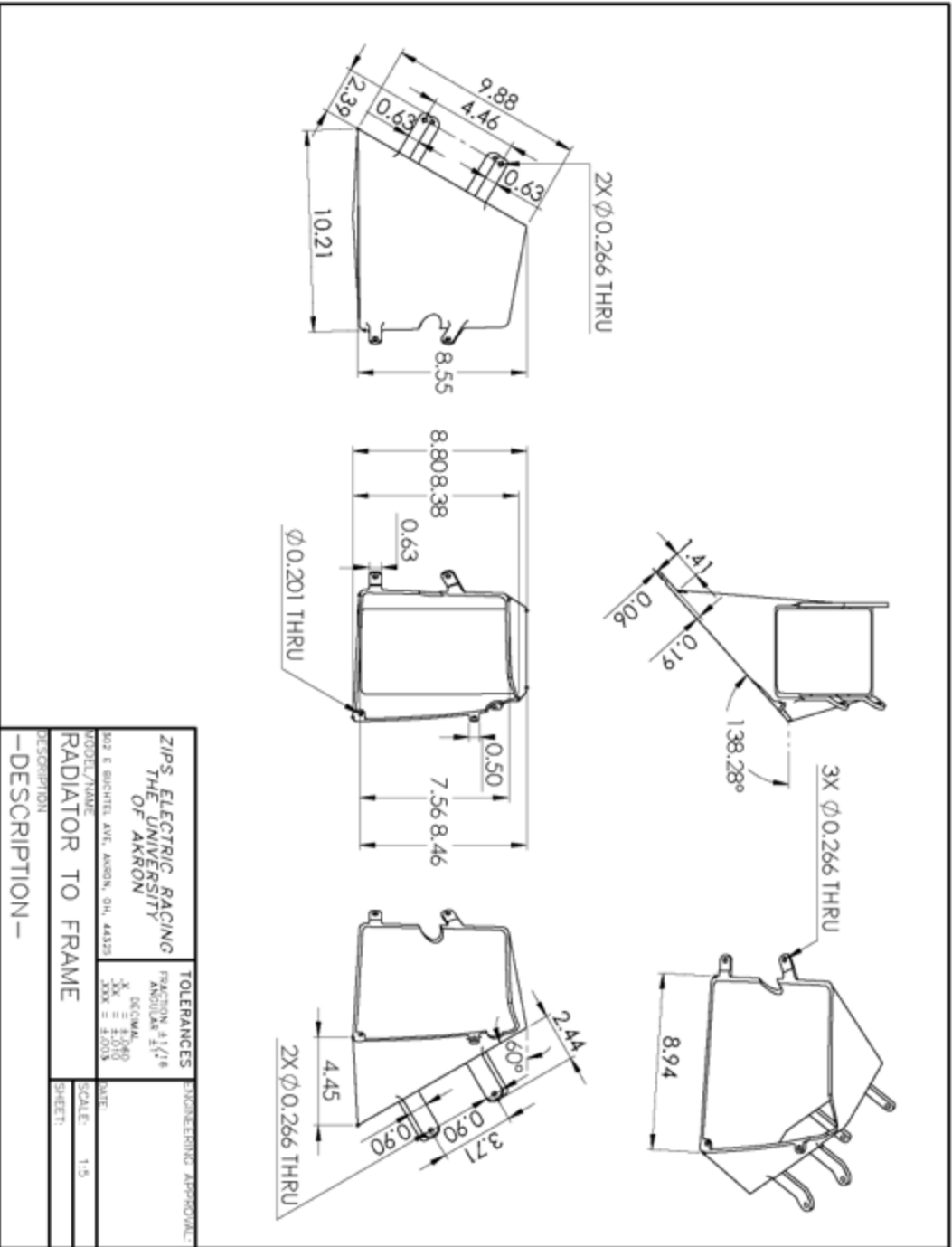


Figure App.E.6: 3D Printed Duct Piece which Connects the Radiator to the Car Frame

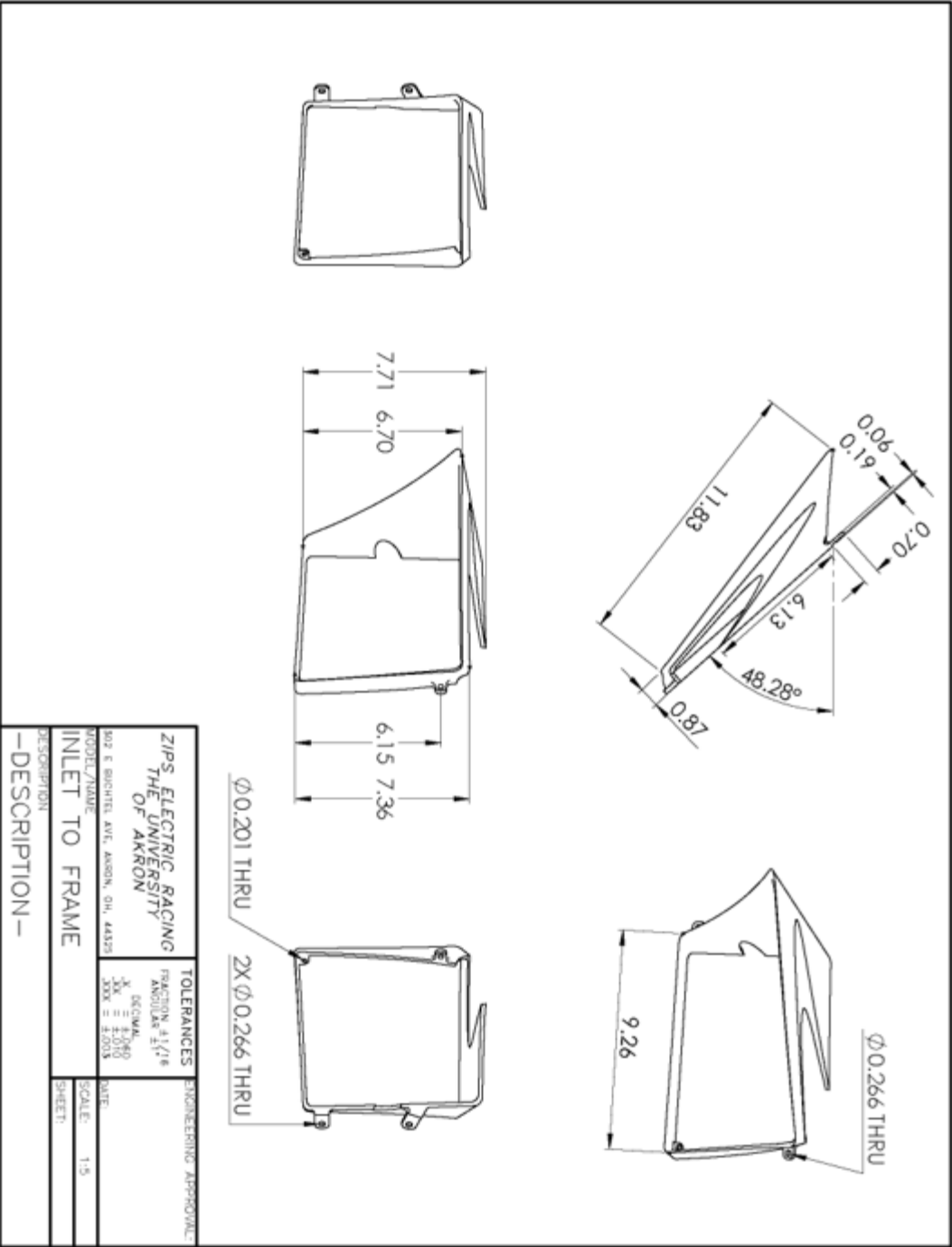


Figure App.E.7: 3D Printed Duct Piece that is the Beginning of the Air Ductwork

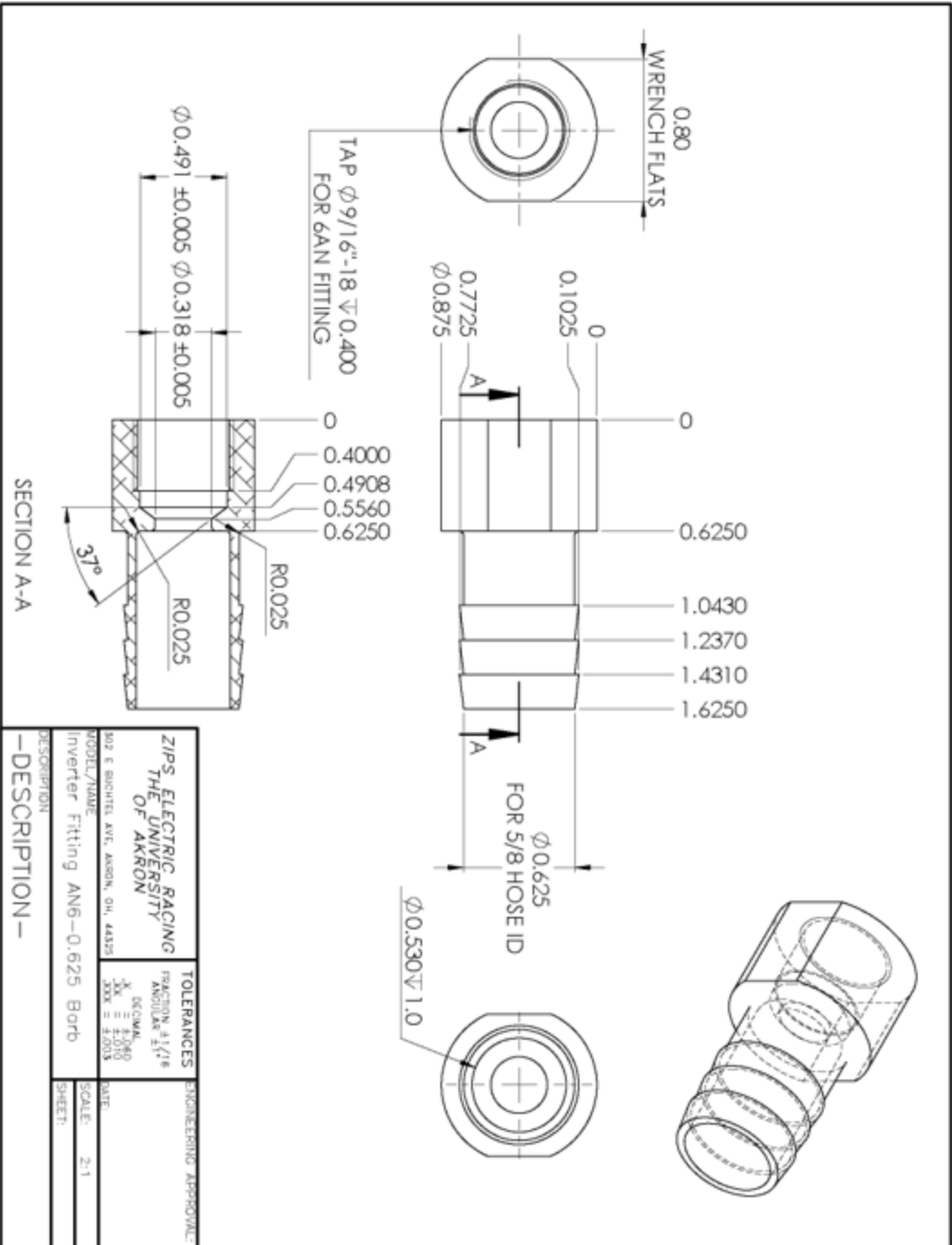
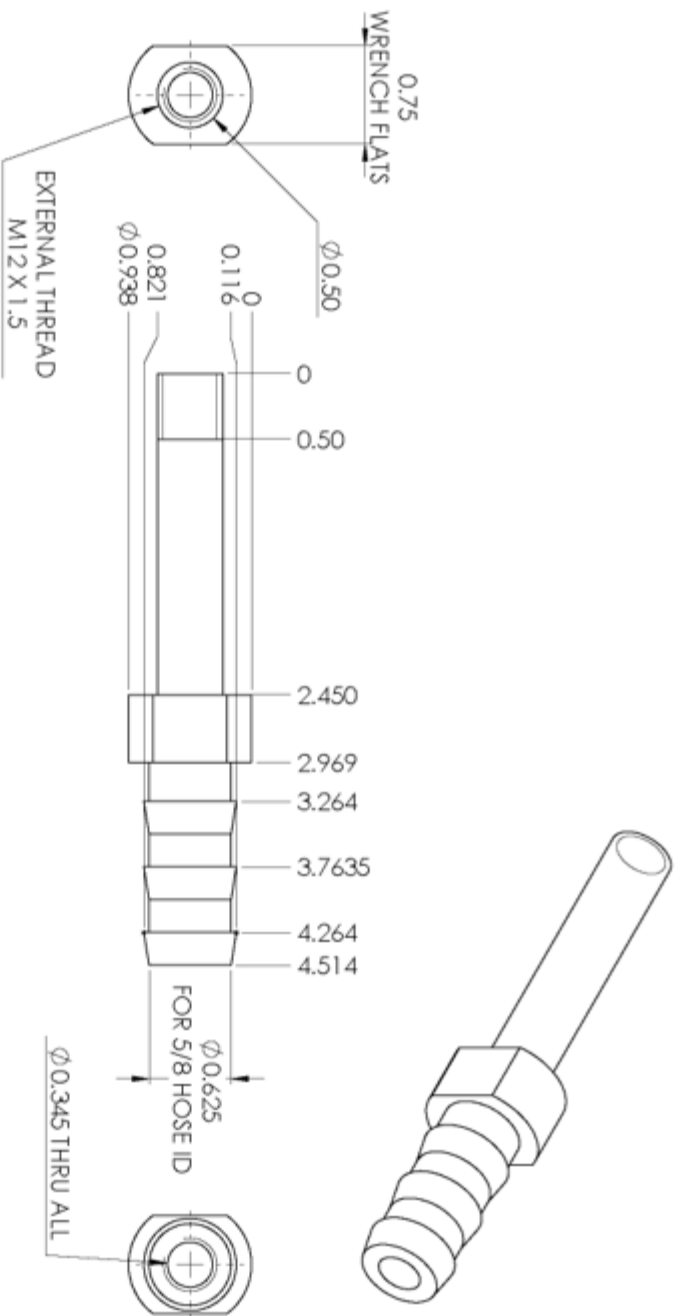


Figure App.E.8: Custom-made Hose Barb for the Inverter



ZIPS ELECTRIC RACING THE UNIVERSITY OF AKRON		TOLERANCES FRACTION 1/16 ANGULAR ±1°	
502 E BRIGHT AVENUE, AKRON, OH, 44325		DECIMAL ±0.005 ±0.010 ±0.015	
MODEL/NAME Motor Coolant Fitting 0.625 Barb		DATE SCALE: 1:1 SHEET:	
DESCRIPTION —			

Figure App.E.9: Custom-made Hose Barb for the Motor

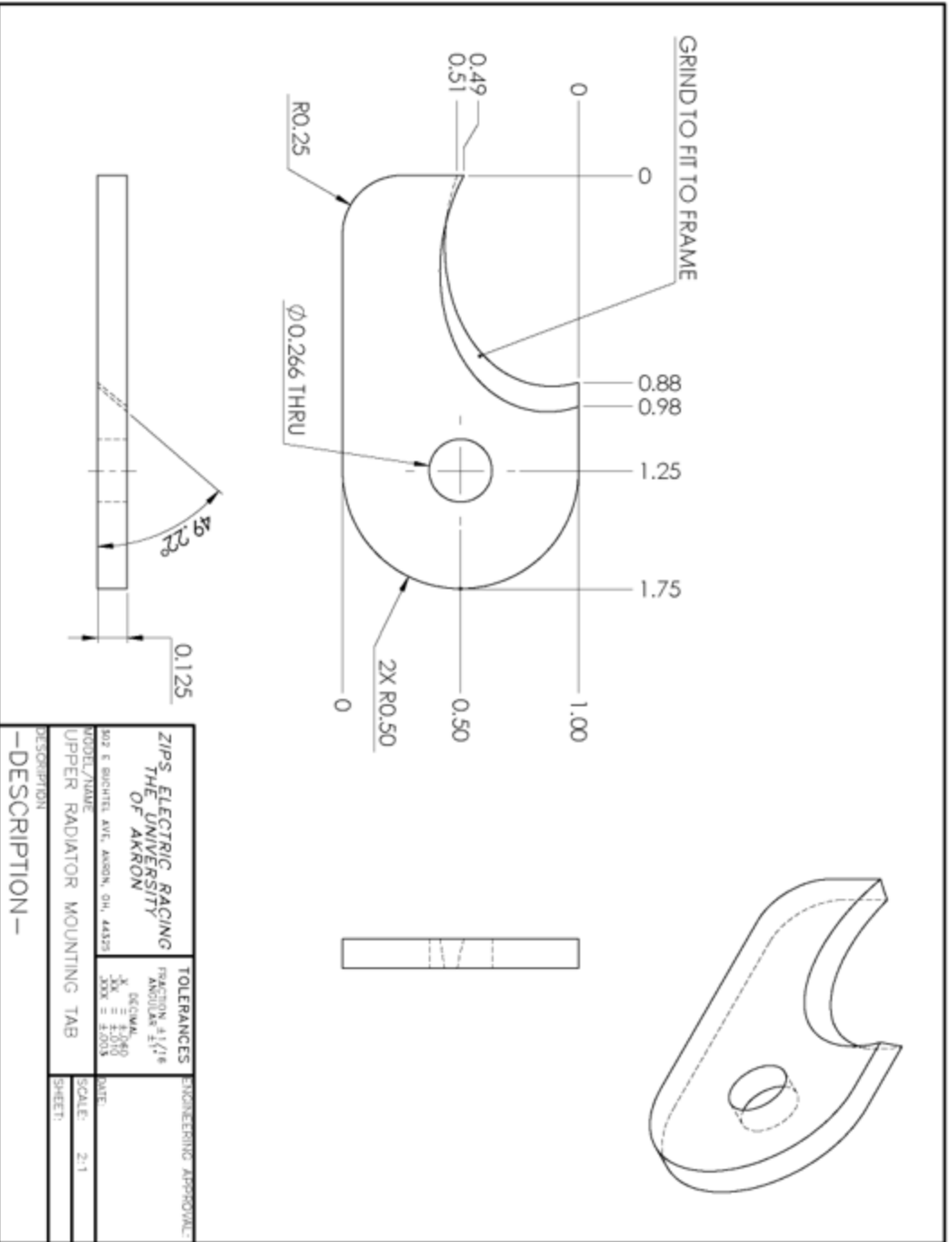


Figure App.E.10: Manufactured Mounting Tab for Radiator

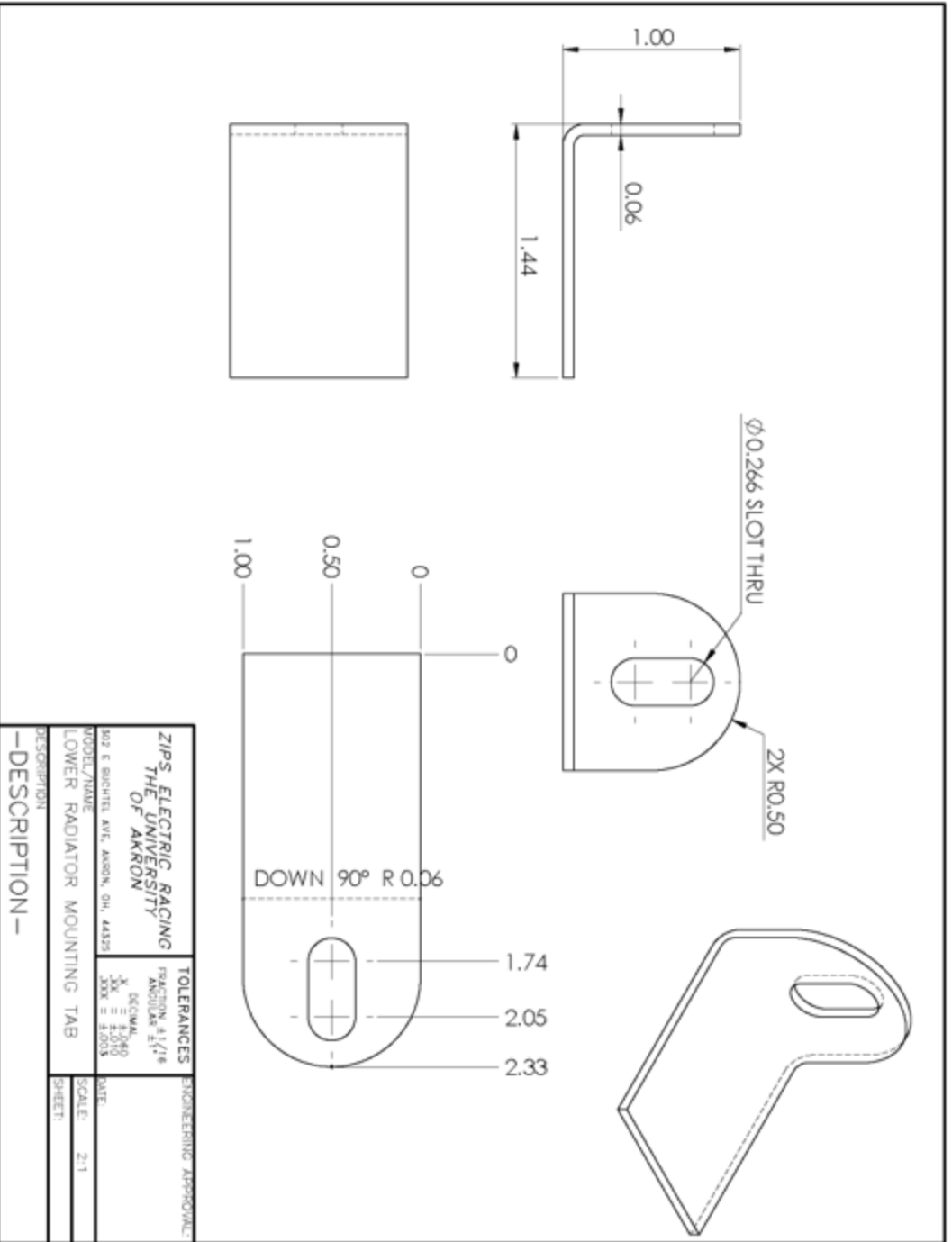
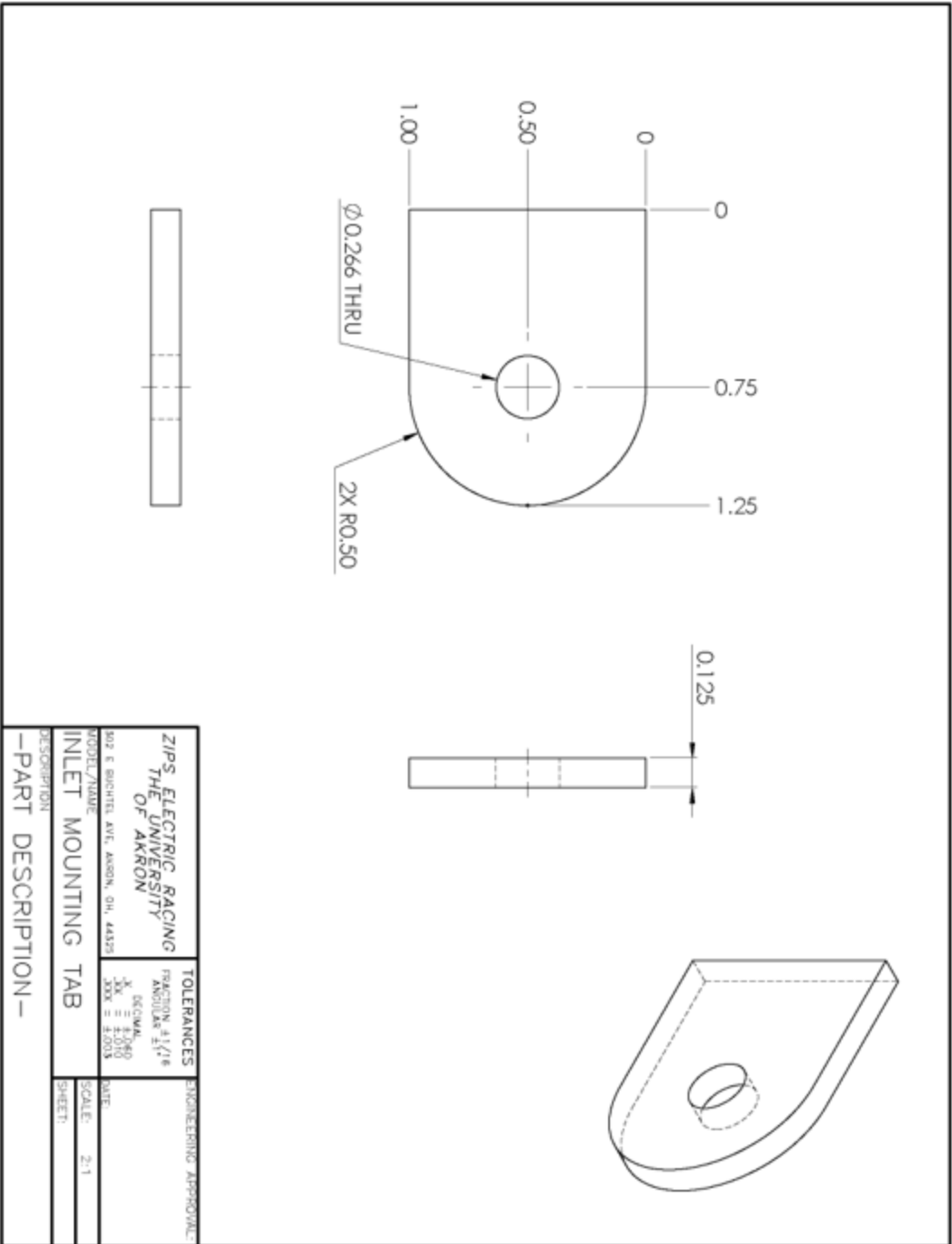


Figure App.E.11: Manufactured Mounting Tab for the Radiator



ZIPS ELECTRIC RACING THE UNIVERSITY OF AKRON		TOLERANCES FRACTION = 1/16 DECIMAL F/100 X XX = ±0.010 XXX = ±0.005		ENGINEERING APPROVAL:	
102 E. BIRCHITE, AVE. AKRON, OH. 44325		DATE:		SCALE: 2:1	
MODEL/TAB/NAME INLET MOUNTING TAB		DESCRIPTION		SHEET:	
-PART DESCRIPTION-		-PART DESCRIPTION-			

Figure App.E.12: Manufactured Mounting Tab for the Duct

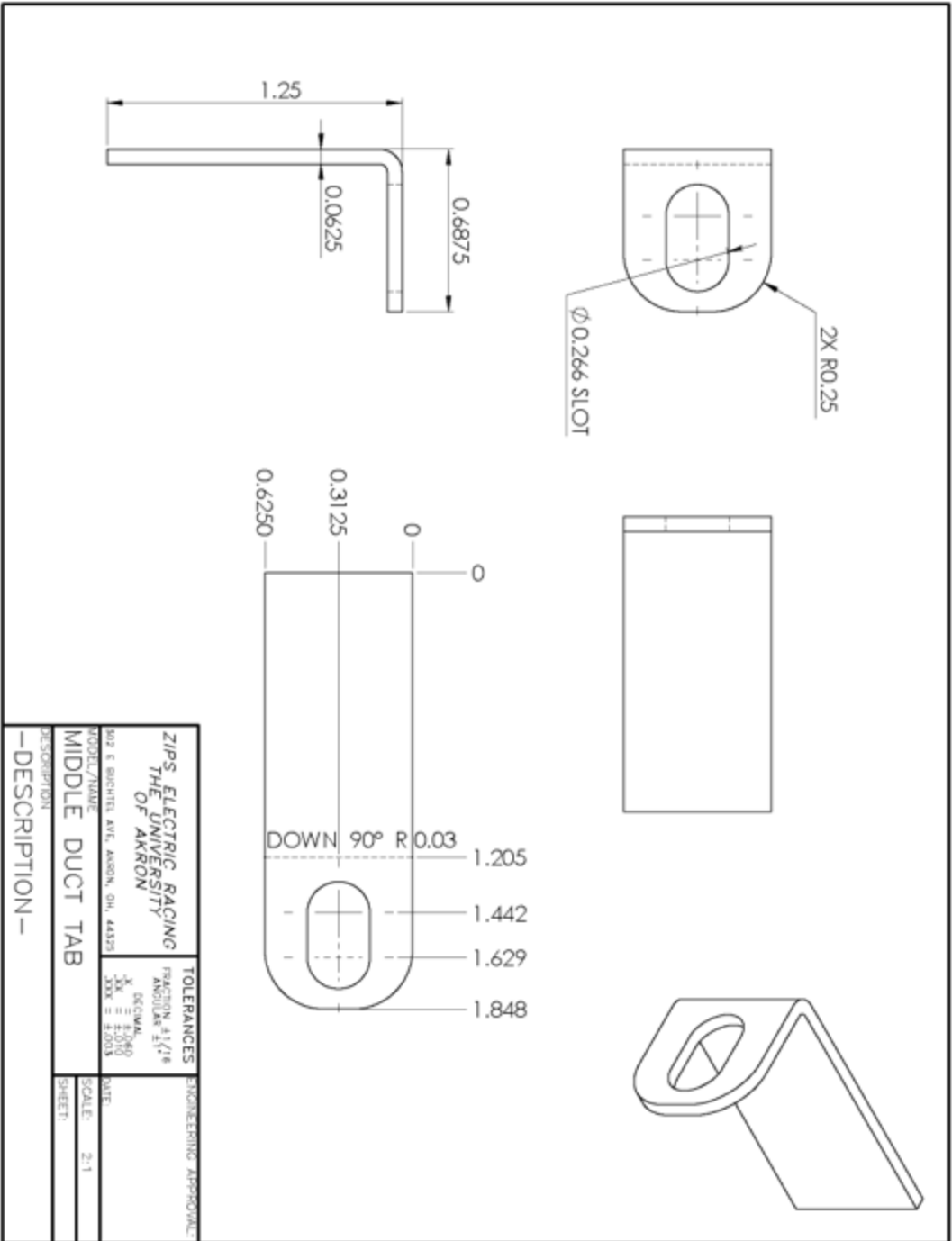


Figure AppE.13: Manufactured Mounting Tab for the Duct

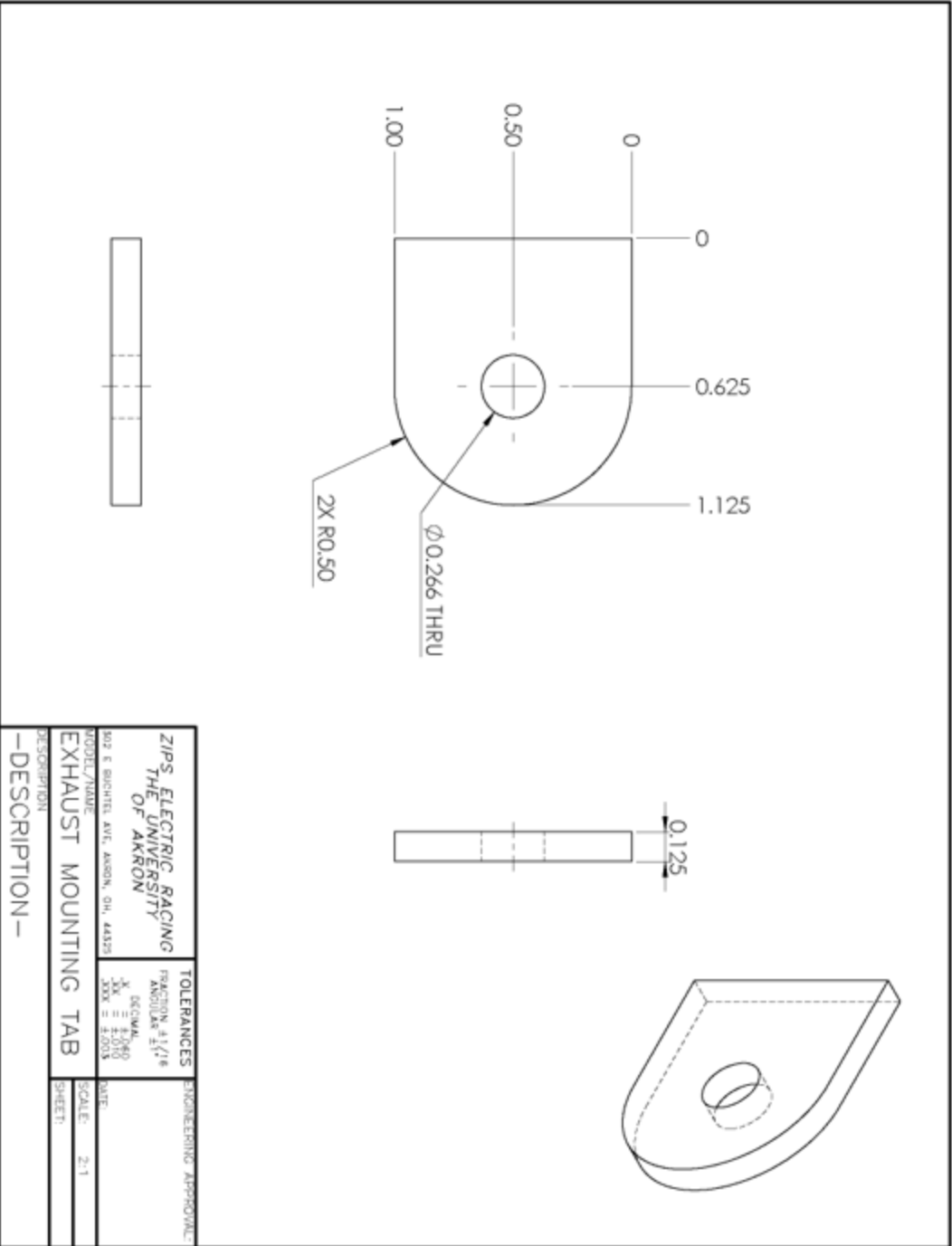


Figure App.E. 14: Manufactured Mounting Tab for the Duct

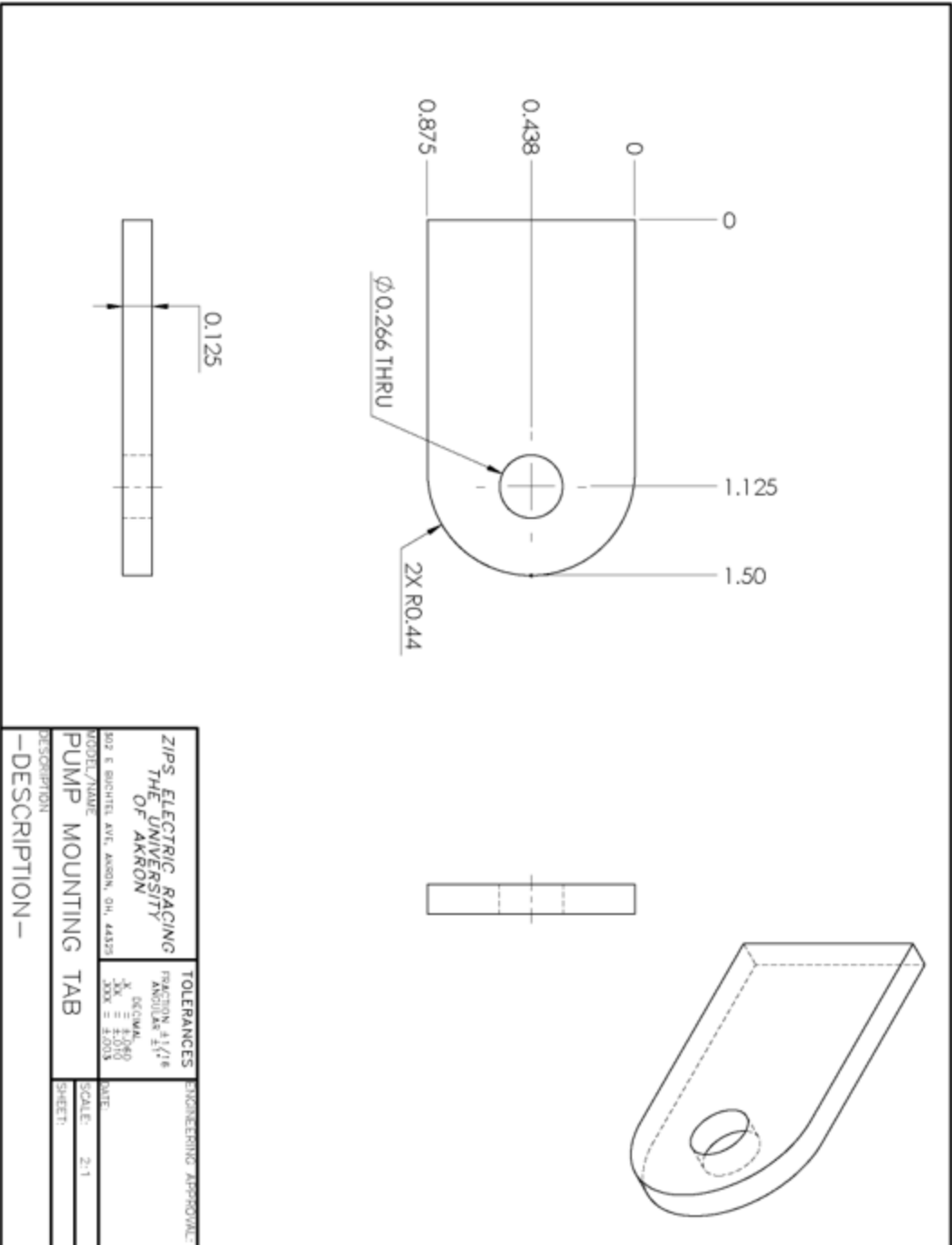


Figure App.E.15: Manufactured Mounting Tab for the Water Pump

Appendix F

Cooling Load Calculation Results

Table App.F.1: Energy required to navigate each turn and/or slalom for the 2012 Lincoln Endurance Track.

Corner	Radius (m)	Velocity (m/s)	Time (s)	Energy (Nm)
1	30.2	23.091	0.775	10605.176
2	12.4	14.796	0.885	7704.711
3	9.9	13.221	0.673	5227.192
4	15.1	16.328	0.741	7126.221
5	20	18.791	0.532	5902.275
6	21.1	19.301	0.632	7204.016
7	188	57.612	0.278	9767.292
8	31.9	23.732	2.141	30114.338
9	40.3	26.674	0.499	7904.655
10	17.7	17.677	0.769	8019.203
11	17.2	17.426	0.918	9432.260
12	19.1	18.363	0.958	10384.082
13	50.8	29.948	0.521	9298.239
14	21.4	19.438	1.096	12579.021
15	15.8	16.702	1.772	17438.511
16	8.3	12.105	1.768	12556.317
17	24.8	20.925	0.755	9343.161
18	13.7	15.552	1.029	9416.639
19	12.4	14.796	0.750	6528.419
20	15.9	16.755	0.734	7246.746
21	22.9	20.107	0.801	9513.704
22	15	16.273	0.498	4770.217
23	13.9	15.665	2.036	18776.303
24	39.1	26.274	1.340	20913.253
25	25.6	21.260	2.404	30226.353
26	52	30.299	0.759	13713.156
27	19.5	18.555	1.741	19060.369
28	10	13.287	0.963	7518.204
29	28.7	22.510	1.319	17587.310
30	17.3	17.477	0.704	7251.374
31	8.8	12.465	1.476	10799.530
32	20.5	19.024	1.046	11747.947
33	8.1	11.958	1.187	8330.676
34	22.5	19.931	1.490	17547.396
35	17.2	17.426	2.709	27825.167
36	20.9	19.209	1.317	14938.267
37	10.9	13.872	1.153	9402.632
38	9.7	13.086	0.978	7516.864

39	10	13.287	1.505	11747.193
40	18.6	18.121	1.247	13331.256
Totals			44.901	486315.647

Table App.F.2. A & B: Summary of acceleration, braking, and maximum velocity in endurance course straight sections.

Straight No.	1	2	3	4	5	6	7
Length (m)	51.3	29.1	47.4	2.5	60	11	13.1
Entrance Velocity (m/s)	18.121	23.732	29.948	15.156	12.105	16.273	26.274
Acceleration Time (s)	1.620	0.779	0.589	0.000	2.408	0.370	0.000
Acceleration Distance (m)	38.112	20.524	18.962	0.000	47.744	6.326	0.000
Acceleration Energy (Nm)	97669.737	53851.238	59080.498	0.000	115112.112	10612.197	0.000
Max Velocity (m/s)	28.934	28.934	34.446	15.156	27.556	17.912	26.274
Max Velocity Distance (m)	4.580	5.017	5.540	0.145	3.152	2.538	6.351
Max Velocity Time (s)	0.158	0.173	0.161	0.010	0.114	0.142	0.242
Max Velocity Energy (Nm)	2364.362	2590.350	3868.523	28.967	1499.450	627.539	2792.940
Braking Time (s)	0.331	0.128	0.850	0.173	0.376	0.127	0.284
Braking Distance (m)	8.608	3.559	22.898	2.355	9.104	2.136	6.749
Exit Velocity (m/s)	23.091	26.674	19.438	12.105	20.925	15.665	21.260

Straight No.	8	9	10	11	12	13	Totals
Length (m)	10.1	30.7	61.6	17.6	6.3	5.9	346.6
Entrance Velocity (m/s)	18.555	22.510	12.465	19.931	19.209	13.872	
Acceleration Time (s)	0.155	0.596	2.352	0.397	0.000	0.000	9.266
Acceleration Distance (m)	2.939	14.514	47.057	8.340	0.000	0.000	204.518
Acceleration Energy (Nm)	5323.174	34822.754	113562.175	17072.320	0.000	0.000	507106.206
Max Velocity (m/s)	19.289	26.179	27.556	22.045	19.209	13.872	
Max Velocity Distance (m)	1.624	5.430	3.290	4.097	1.301	5.300	48.365
Max Velocity Time (s)	0.084	0.207	0.119	0.186	0.068	0.382	2.047
Max Velocity Energy (Nm)	444.898	2373.594	1565.154	1365.463	354.254	955.770	20831.262
Braking Time (s)	0.340	0.493	0.483	0.262	0.302	0.045	4.193
Braking Distance (m)	5.537	10.757	11.253	5.163	4.999	0.600	93.718
Exit Velocity (m/s)	13.287	17.477	19.024	17.426	13.872	13.086	

Appendix G

Weighted Decision Matrices

Table App.G.1: Weighted decision matrix for using ABS ducting

Cooling Ductwork (ABS)			
Evaluation Criteria	Weight Factor	Score (11-Point)	Rating
Material Cost	0.2	10	2
Manufacturing Cost	0.2	7	1.4
Repair Cost	0.1	3	0.3
Durability	0.24	8	1.92
Weight	0.25	10	2.5
Production Time	0.05	9	0.45
			8.57

Table App.G.2: Weighted decision matrix for using sheet metal ducting

Cooling Ductwork (Sheet Metal)			
Evaluation Criteria	Weight Factor	Score (11-Point)	Rating
Material Cost	0.2	7	1.4
Manufacturing Cost	0.2	6	1.2
Repair Cost	0.1	5	0.5
Durability	0.24	9	2.16
Weight	0.25	1	0.25
Production Time	0.05	6	0.3
			5.81

Table App.G.3: Weighted decision matrix for using fiberglass ducting

Cooling Ductwork (Fiberglass)			
Evaluation Criteria	Weight Factor	Score (11-Point)	Rating
Material Cost	0.2	9	1.8
Manufacturing Cost	0.2	4	0.8
Repair Cost	0.1	4	0.4
Durability	0.24	4	0.96
Weight	0.25	8	2
Production Time	0.05	3	0.15
			6.11

Table App.G.4: Weighted decision matrix for using aluminum tubing

Cooling Line Tubing (Aluminum)			
Evaluation Criteria	Weight Factor	Score (11-Point)	Rating
Material Cost	0.2	6	1.2
Manufacturing Cost	0.2	5	1
Repair Cost	0.1	4	0.4
Durability	0.24	7	1.68
Weight	0.25	6	1.5
Production Time	0.05	5	0.25
			6.03

Table App.G.5: Weighted decision matrix for using silicone tubing

Cooling Line Tubing (Silicone)			
Evaluation Criteria	Weight Factor	Score (11-Point)	Rating
Material Cost	0.2	6	1.2
Manufacturing Cost	0.2	9	1.8
Repair Cost	0.1	6	0.6
Durability	0.24	7	1.68
Weight	0.25	9	2.25
Production Time	0.05	10	0.5
			8.03

Table App.G.6: Weighted decision matrix for using PVC tubing

Cooling Line Tubing (PVC)			
Evaluation Criteria	Weight Factor	Score (11-Point)	Rating
Material Cost	0.2	7	1.4
Manufacturing Cost	0.2	5	1
Repair Cost	0.1	4	0.4
Durability	0.24	6	1.44
Weight	0.25	7	1.75
Production Time	0.05	5	0.25
			6.24